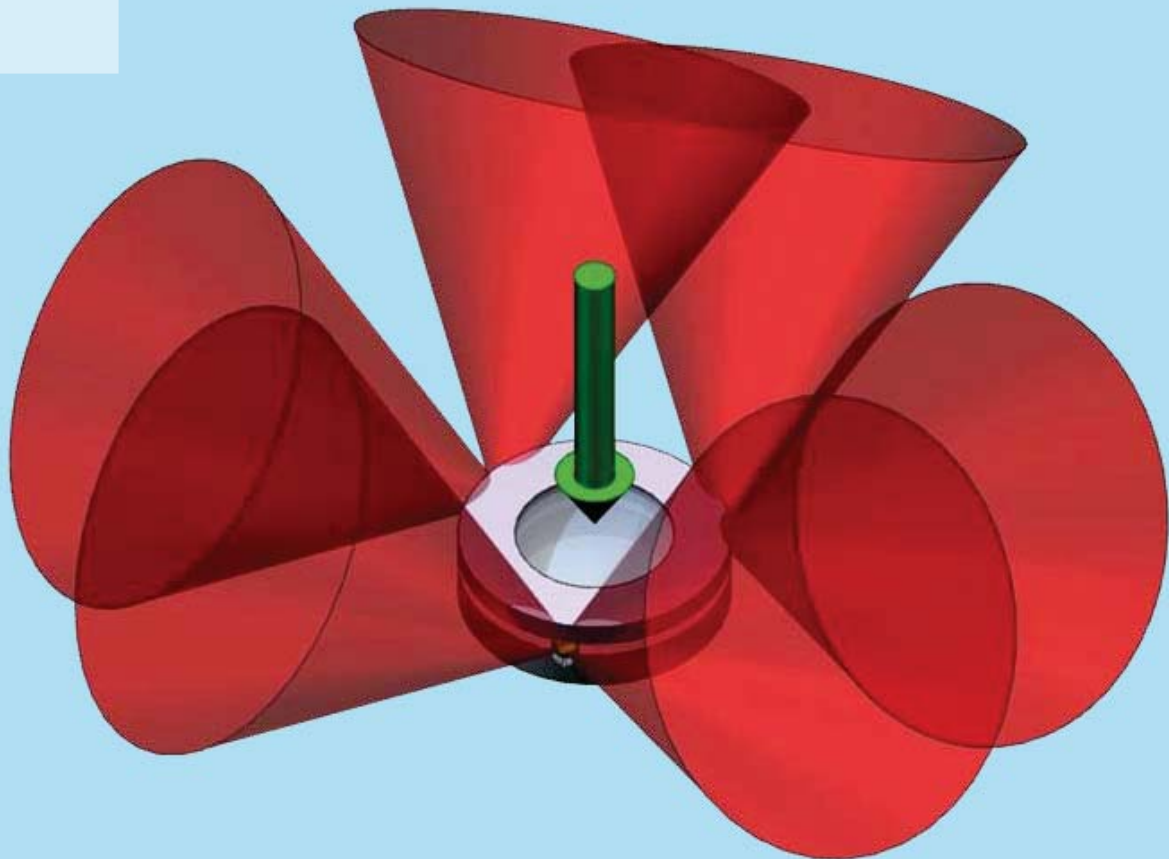


PROFESSIONAL JOURNAL ON PRECISION ENGINEERING

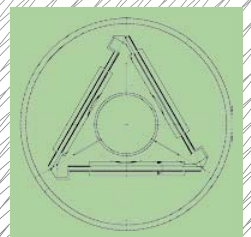
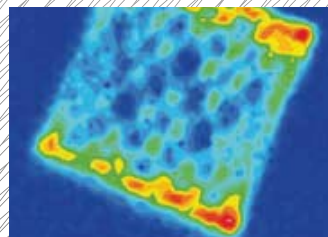
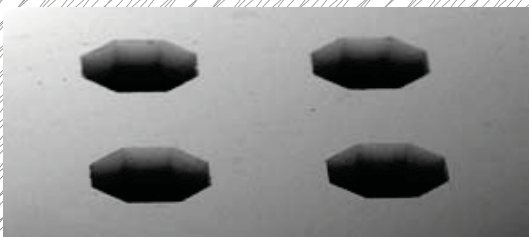
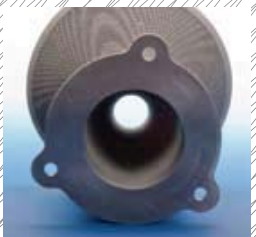


MIKRONIEK

ISSUE 1
2013
(VOL. 53)



- OPTIMUM FLEXURE **LINEAR GUIDANCE** ■ REFLECTIONS ON **SELF-ALIGNMENT**
- **ACTUATORS:** RELUCTANCE VS LORENTZ ■ **VACUUM-COMPATIBLE** WAFER STAGE



Mikroniek is a publication of the DUTCH SOCIETY FOR PRECISION ENGINEERING www.dspe.nl

DSPE

24 and 25
April 2013
Klokgebouw
Eindhoven, NL



HIGH-TECH SYSTEMS

International Conference and Exhibition on Mechatronics and Precision Technology

Exhibitors

AAE
Alten Mechatronics
ASML
Beckhoff.nl / IAL
BKL Engineering
Brainport Industries
CCM Centre for Concepts in Mechatronics
Ceratec Technical Ceramics
Claytex Services
Controllab Products
DEMCON advanced mechatronics
DSPE
Dutch Precision Technology
Eltromat
Enterprise Europe Network / Syntens
Festo
Framo Morat
Frencken Europe
Greentech Engineering
HEIDENHAIN
Hittech Group
IBS Precision Engineering
Irmato Industrial Solutions
Janssen Precision Engineering
KMWE Precisie Eindhoven
LEMO Connectors Benelux
Maséon Technology
MathWorks
maxon motor benelux
MTA
MTSA Technopower
National Instruments
Nijdra Special Products
Nobleo Technology
NTS-Group
Ocê-Technologies
Philips Innovation Services
PM-Bearings
Prodrive
Reden
Technologiestichting STW
Tecnotion
Telerelex
TEVEL Components
The High Tech Institute
TMC Group
TNO
Variass
Vernooy Vacuum Engineering
Yacht
Yokogawa

Exhibition and Conference on Mechatronics and Precision Technology

On 24 and 25 April 2013 Brainport Industries, DSPE, FMTC, Syntens and Techwatch organise the exhibition and conference High-Tech Systems (successor of Hightech Mechatronica).

This event focusses on designers, technical managers and developers of mechatronic systems.

Themes technical conference programme:

- Agro & food
- Medical systems
- Automotive
- Semicon
- International collaboration (management)

Registration open

You can now register for High-Tech Systems 2013. Entrance to the exhibition and conference programme is free of charge when you register before 19 April 2013.
www.hightechsystems.eu/visitors.

Sponsor

PHILIPS

Also at High-Tech Systems:

End symposium research programme SmartPie

End symposium research programme SmartPie, provided by the foundation Applied Piezo.

Model-Driven Development Days

Parallel to High-Tech Systems, Techwatch organises their annual Model-Driven Development Days with an interesting conference programme on finite elements, multi-body dynamics, multi-physics development methods and simulation as well as model-based software and system development and testing.

Programme international guests

Invite your international relations to participate on 23 April (prior to High-Tech Systems) in one of the **four unique** tours along high-tech companies and institutes in the regions Eindhoven and Leuven. The guests can visit companies and institutes like ASML, FMTC, Frencken, Holst Centre, MuTracx, Shapeways, imec, KU Leuven, NTS, NXP, Philips Innovation Services, TNO and VDL-ETG.

www.hightechsystems.eu/programme

High-Tech Systems is the result of a collaboration between Brainport Industries, Dutch Society for Precision Engineering, Syntens Innovatiecentrum, FMTC and Techwatch, publisher of Bits&Chips and Mechatronica&Machinebouw

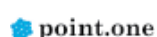


High-Tech Systems 2013
is supported by



www.hightechsystems.eu

#HTS13



PUBLICATION INFORMATION

Objective

Professional journal on precision engineering and the official organ of DSPE, the Dutch Society for Precision Engineering. Mikroniek provides current information about scientific, technical and business developments in the fields of precision engineering, mechatronics and optics.

The journal is read by researchers and professionals in charge of the development and realisation of advanced precision machinery.



Publisher

DSPE
High Tech Campus 1, 5656 AE Eindhoven
PO Box 80036, 5600 JW Eindhoven
info@dspe.nl, www.dspe.nl

Editorial board

Ir. Herman Soemers (chairman, University of Twente, Philips Innovation Services), ir.ing. Bert Brals (CCM), dr.ir. Dannis Brouwer (University of Twente), ir. Bart Dirkx (WittyWorX), ir. Jos Günsing (Marome-Tech, Avans), ir. Rob van Haendel (Philips Innovation Services), ir. Huub Janssen (Janssen Precision Engineering), ir. Henk Kiela (Opteq, Fontys), ir. Casper Kruijer, MBI (FEI), ing. Ronald Lamers, M.Sc. (MI-Partners), ir. Piet van Rens (Settels Savenije van Amelsvoort), ir. Ad Vermeer (SolayTec, Adinsyde)

Editor

Hans van Eerden, hans.vaneerden@dspe.nl

Advertising canvasser

Sales & Services
+31 (0)229 – 211 211, gerrit@salesandservices.nl

Design and realisation

Twin Media bv
PO Box 317, 4100 AH Culemborg (NL)
+31 (0)345 – 470 500, info@twinmediabv.nl

Subscription costs

The Netherlands	€ 70.00 (excl. VAT) per year
Europe	€ 80.00 (excl. VAT) per year
Outside Europe	€ 70.00 + postage (excl. VAT) per year

Mikroniek appears six times a year.

© Nothing from this publication may be reproduced or copied without the express permission of the publisher.

ISSN 0026-3699



The main cover photo (graphical method for determining optimal design of self-aligning kinematic mount) is courtesy of Settels Savenije van Amelsvoort.

IN THIS ISSUE

ISSUE 1
2013

05

The optimum flexure linear guidance

The positive properties of flexure guidances are extended with those of relatively large excursions.

12

Reflections on self-alignment

A self-aligning kinematic mount has been designed for an optical component with high stiffness and high repeatability.

15

Actuators: Reluctance vs Lorentz

A brief comparative analysis of two types of electro-magnetic actuators, emphasising their specific working principle and their advantages and disadvantages.

22

Precision Fair 2012 impressions

The Precision Fair 2012 showed much more manufacturing and measuring stands than ever before.

27

ALM parts in space

European Space Agency investigates Additive Layered Manufacturing.

30

Design for vacuum: Through the wall

A stage design featuring a low degree of complexity and minimising contamination of the vacuum: the so-called through-wall stage.

36

Exciting international mechatronics event

High-Tech Systems 2013 preview.

38

Innovative technical ceramic solutions

Ceramic Injection Moulding and 3D printing technique.

40

Novel turret optics design

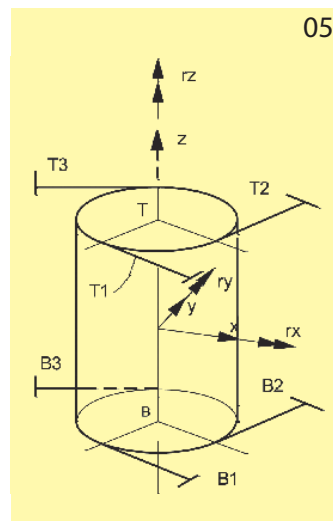
Development of an automatic multi-wavelength laser delivery solution based on micropositioning systems and motion controls.

43

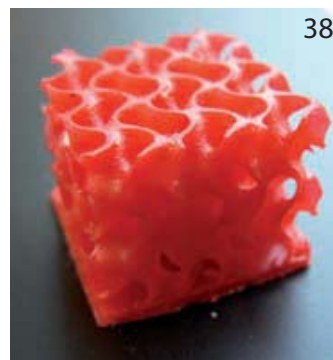
Precision joining of plastics and metals

Report on Micro-joining seminar.

05



38



FEATURES

04 EDITORIAL

Bart Dirkx, co-ordinator of Mikroniek editorial board, on the new look and feel.

21 DSPE

Constructor Award for robot hand design.

48 CPE COURSE CALENDAR

Overview of Certified Precision Engineer courses.

49 UPCOMING EVENTS

Including: Zuid-Holland Instrumentation Event 2013.

50 NEWS

Including: Book review of "Infrared Thermal Imaging".

EDITORIAL

NEW LOOK AND FEEL

It is my pleasure to present to you Mikroniek's new look and feel. But first I want to share a bit of history. Mikroniek dates back to 1961, when it started as "Fijntechniek" (Precision Technology), the journal of the N.V.F.T. (Nederlandse Vereniging voor Fijnmechanische Techniek). In 1967 its name was changed into Mikron, but after a protest from the Swiss company Mikron it was changed into Mikroniek in 1968. Mikroniek is the combination of "Mikron" (the Greek word for small, e.g. as used in micrometer) and "kroniek" (Dutch for chronicle). The original aim was to present a chronological history of the development of precision technology. The current objective still is to be a journal whose technological content is so interesting that you would rather keep it than throw it away after reading.

Mikroniek has seen some big changes over the years. In 2007, its layout design went from black/white to colour. And after gradually introducing English language articles, it was decided in 2009 to switch to English entirely. Business has become more international over time, and the same holds for R&D. Even within the Netherlands, English is becoming the language of choice in scientific and business communities.

Times change and so have the expectations of Mikroniek readers. Information has become ubiquitous. Besides the content itself, the presentation determines whether the target audience can be reached. We felt it was time, therefore, to align the look and feel of Mikroniek to meet the current standards of professionalism and quality that our readers expect from a DSPE journal. Of course, the format alone does not make for a good article, but it does make it a pleasure to read. This connects to what Mikroniek stands for: high-quality technical, yet readable, articles complemented with information about the high-precision ecosystem for a wide audience of technically engaged people.

One thing to argue about is whether the use of the term Mikron/micron in Mikroniek still holds water in a world of ever-increasing accuracy. Microchips are currently produced to the nanometer scale and Atomic Force Microscopes measure materials to atomic resolution level. On the other hand, Mikroniek is not only about the highest accuracy and new technologies are always entering the micrometer domain. Hence we have decided to hold on to the name Mikroniek, with its own Dutch signature in a global ecosystem.

I hope you enjoy the new look and feel of Mikroniek. By making sure that it is an attractive journal to read, we hope to reward all the volunteers who have contributed to Mikroniek. It is also an invitation to others to write that special article that is indeed worth keeping.

*Bart Dirkx, M.Sc., EM-BI
Co-ordinator Mikroniek Editorial Board
Founder and Managing Director of WittyWorX*

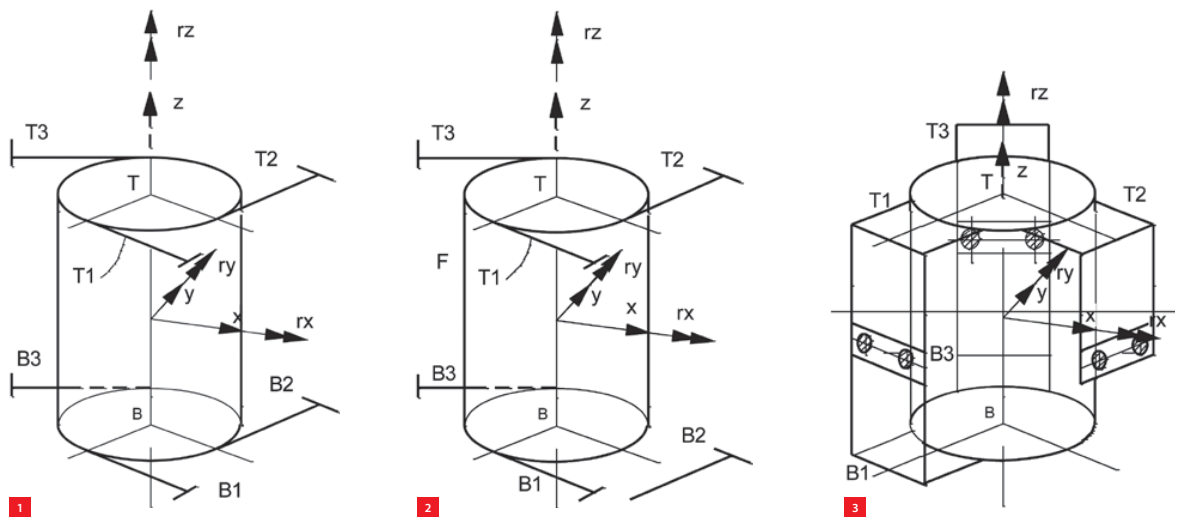


THE OPTIMUM FLEXURE LINEAR GUIDANCE

Linear guidances are usually based on rolling bodies and linear races. Their accuracy, in terms of tilt and linearity, depends on the precision of races and rollers. Extreme accuracy, e.g. required in optical applications, can be achieved by means of flexible elements. However, in general their excursions are limited. Here, the positive properties of flexure guidances – extreme linearity, near-zero tilt, absence of friction, no need for lubrication – are extended with that of relatively large excursions.

RIEN KOSTER

- 1 Overconstrained flexure guidance.
- 2 A 1-DoF flexure linear guidance.
- 3 Folded leaf-spring flexures [1].



State-of-the-art linear guidance with flexures

The moving body TB (Figure 1) has one degree of freedom (DoF): its linear travel z along the center line. Five coordinates (x, y, rx, ry, rz) have to be constrained. In favour of the accuracy of the guidance, the top plane T and the bottom plane B both should be rotationally symmetrical. This symmetry could be provided by three flexures (wires or beams T1,2,3) in the top plane T and three flexures (B1,2,3) in the bottom plane B. The body TB, however, would be overconstrained, because both in the top plane T and in the bottom plane B the rotation coordinate rz would be constrained.

The result would be that one of the flexures were in the state of buckling and therefore hardly have any stiffness in its

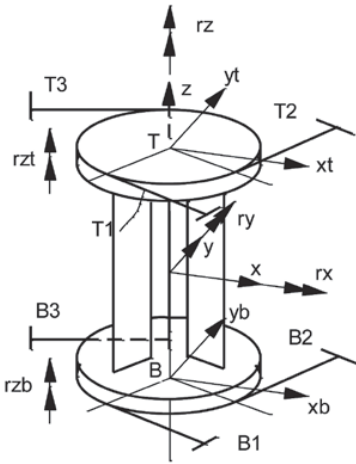
longitudinal direction. Figure 2 illustrates how to avoid this last problem: one of the flexible elements (B2) has been removed. Now the moving body TB is constrained by means of five bars; five coordinates (x, y, rz, ry, rz) are constrained, one DoF (z) remains.

Due to the finite length of the flexures T1,2,3 and B1,2,3, however, the rotation rz , although constrained, is non-zero. If this inevitable rotation is not allowed in the particular application, the five bars or wire flexures are replaced by five folded leaf-springs (Figure 3) [1]. Unfortunately, the problem of rotational asymmetry has not been solved. The above concepts are, in general, intended for relatively small excursions, i.e. a few percent of the outer dimension of the set-up, such as optical focusing provisions.

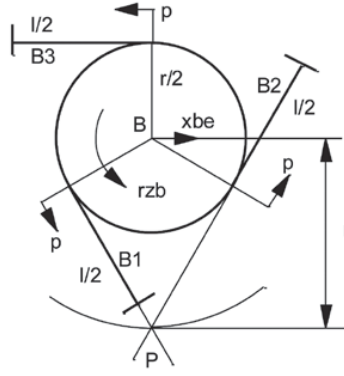
AUTHOR'S NOTE

Prof. dr ir M.P. (Rien) Koster is director of KEI Koster Eindhoven Innovator, consultant Mechanical Engineering Design and Mechatronics.

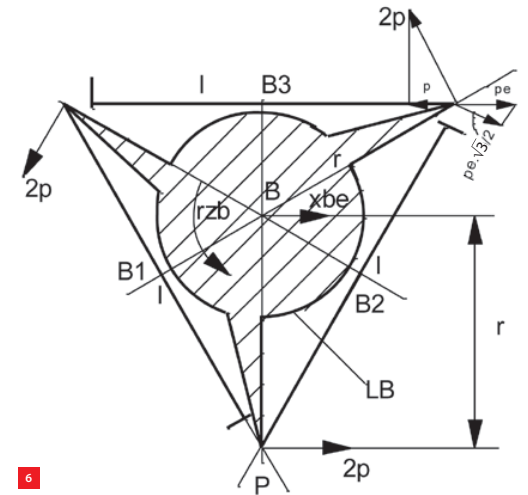
kei@onsneteindhoven.nl



4



5



6

4 Torsionally flexible body TB.

5 Average-length flexures.

6 Maximum-length flexures.

Large-excursion flexure linear guidance

In a particular application the requirement came up for an excursion as high as 20% of the outer dimension. An additional requirement was that the body should oscillate at a frequency of about 50 Hz. In that case the question arises to what extent the excursion can be increased and what the consequences are.

Degrees of freedom

For ultimate linearity of the guidance no asymmetry is allowed. Therefore, we return to the lay-out of Figure 1. The problem of the overconstrained coordinate rz will be solved by modifying the cross section of the moving body TB (Figure 4) in such a way that its torsion stiffness around the center line is relatively low, while leaving all the body's other stiffnesses unchanged. In the plane T the flexures T1,2,3 constrain the coordinates x_t, y_t, rz_t ; in the plane B the flexures B1,2,3 constrain the coordinates x_b, y_b, rz_b . Hence, six coordinates of the body (x, rx, y, ry, rz_b, rz_t) are constrained by six flexures. No overconstraint exists, one DoF (z) remains.

It should be emphasised that any excursion in the free direction z will be accompanied by an inevitable rotation ($rz_t = rz_b = rz$).

Flexures

The longer the flexures, the larger the allowed excursion z before the maximum bending stress will be reached. Keeping the outer diameter $2r$ (Figures 5 and 6) equal, the length l of the flexures of Figure 6 is about twice that of Figure 5. The bending stress will decrease with a factor of 4.

An additional advantage of the configuration of Figure 6 is that the virtual retraction p (Figure 7) due to the z -excursion and – as a consequence – the angles of

deflection of the flexures, in the T- and the B-plane, will be minimised.

The virtual retraction is equal to

$$p = \hat{z}^2 / (2s)$$

where \hat{z} is the amplitude of the z -excursion and s is the length of the flexure.

Figure 5 yields:

$$s = l / 2 \approx (r / 2) \sqrt{3} \quad (1)$$

$$p \approx \frac{\hat{z}^2}{r \sqrt{3}} \quad (2)$$

The angle of rotation of the body, hence the angle of deflection of the flexure is equal to

$$rz = \frac{p}{r / 2} = \frac{2\hat{z}^2}{r^2 \sqrt{3}} \quad (3)$$

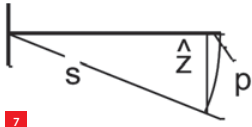
Figure 6 yields:

$$s = l = r \sqrt{3} \quad (4)$$

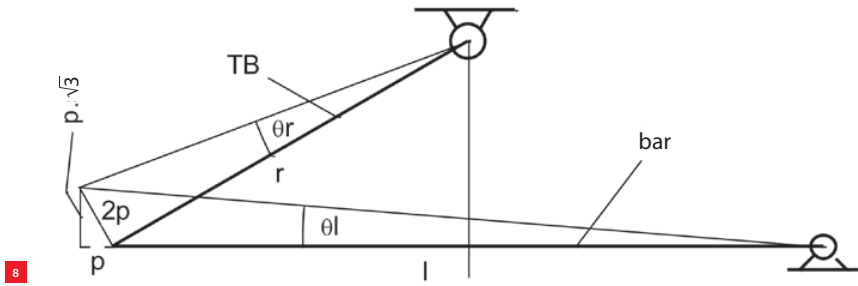
$$p \approx \frac{\hat{z}^2}{2r \sqrt{3}} \quad (5)$$

The angle of rotation of the flexure with respect to the frame (Figure 8) is equal to

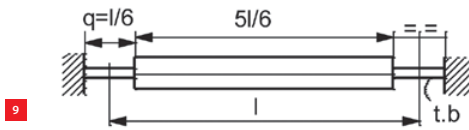
$$\theta_i \approx \frac{p \sqrt{3}}{l} = \frac{p \sqrt{3}}{r \sqrt{3}} = \frac{\hat{z}^2}{2r^2 \sqrt{3}} \quad (6a)$$



7



8



9

7 Virtual retraction p.

8 Angles of rotation flexures (configuration of Figure 6).

9 Optimum flexure.

The angle of rotation of the flexure with respect to the body (Figure 8) is equal to

$$\theta_n \approx \theta_r - \theta_l = \frac{2p}{r} - \frac{p}{r} = \frac{\hat{z}^2}{2r^2\sqrt{3}} \quad (6b)$$

The angles of rotation (Expression 6b) are only $\frac{1}{4}$ of the angle from Expression 3. Since the bending stresses are direct proportional to these angles, it is stated that the configuration of Figure 6 reduces the in-plane bending stresses in the flexures by a factor of 4 with respect to the configuration of Figure 5. Obviously, θ_l and θ_n are equal!

The optimum flexure

The flexures T1,2,3 and B1,2,3 (Figure 4) are of the bar type. From the point of view of longitudinal stiffness, lateral flexibility and buckling load capacity, the configuration of Figure 9 [1] is preferred. If the effective length is equal to l , the rigid part has a length of $5l/6$, whereas the flexible parts each have a length of $q = l/6$.

In that case the bar of Figure 9 yields:

$$\text{longitudinal stiffness } c_{\text{long}} = \frac{3EA}{l} \quad (7)$$

$$\text{lateral stiffness } c_{\text{lat}} \approx \frac{12EI}{l^3} \quad (8)$$

$$\text{buckling limit } F_k \approx \frac{36EI}{l^2} \quad (9)$$

$$\text{bending stress } \sigma_b \approx \frac{3Et\theta}{l} \quad (10)$$

where θ is the bending angle of the flex part of the bar and t is the thickness.

Concept of linear guidance

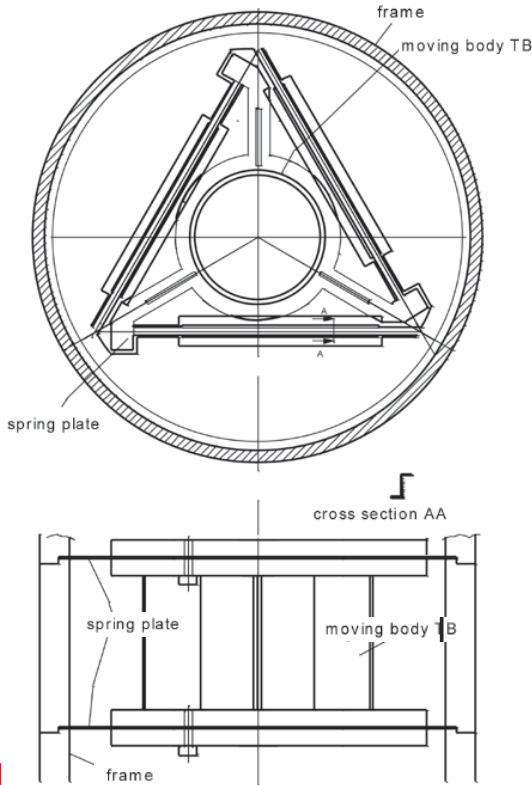
The ingredients maximum-length flexures (Figure 6) and optimum flexure (Figure 9) are combined in the concept of the spring plate of Figure 10. Here, the flexures have been shaped by cutting gaps into a sheet of high-tensile-strength alloy. Suitable manufacturing processes are spark erosion, laser cutting and etching. In order to get identical spring plates, two sheets are manufactured on top of each other. The flexures connect the outer contour, fitted to the frame, with the inner part, fitted to the moving body TB. The moving body itself consists of a top and a bottom flange to which the spring plates are clamped, and a central section with low torsion stiffness, according to the idea of Figure 4.

Attention should be given to the configuration of the cross section AA (Figure 10) of the rigid part. Its center line coincides with those of the flexible parts, in order to avoid a bending moment in the bar when loaded along the center line. Folding into the depicted profile should take place in advance to the heat treatment of the spring plate.

In the actual case of Figure 10 the spring plate's outer diameter was 200 mm, the amplitude of the moving body was $\hat{z} = 15$ mm to either side from the zero position. The spring plate thickness was $t = 0.6$ mm. The bending stress is the critical parameter in the design of the spring plate. It consists of two contributions.

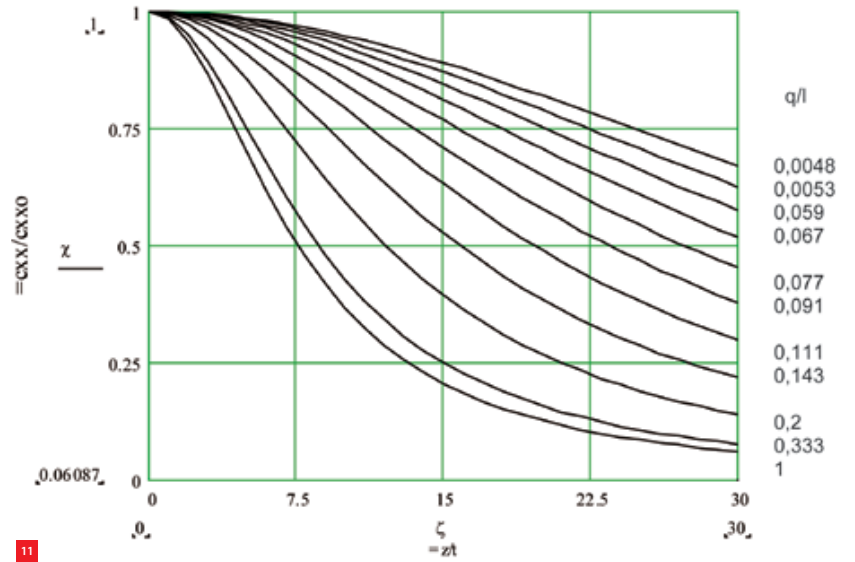
The deflection in the z-direction generates a stress (Expression 10) equal to

$$\sigma_z = \frac{3\hat{z}Et}{l^2} \approx 400 \text{ N / mm}^2$$



10 Concept of linear guidance.

11 Longitudinal stiffness of a bar (c_{xx}) relative to its zero-deflection stiffness (c_{xx0}) as a function of the relative deflection z/t , with the flex part q/l as a parameter, and in the case of rectangular cross sections.



The deflection due to the rotation (θ_r , Figure 8) generates a bending stress equal to

$$\sigma_\theta = \frac{3\hat{\theta}_r E b}{l} \approx 160 \text{ N/mm}^2$$

where the width of the flex part is $b = 4 \text{ mm}$. The addition of the two should not exceed the fatigue strength of the applied material.

Lateral stiffness of the linear guidance

The lateral stiffness of the moving body with respect to the frame is determined by the flexures. The longitudinal stiffness of a flexure (Expression 7) predominates its lateral stiffness (Expression 8) to a high extent. The longitudinal stiffness of the bars (Figure 9) determines the lateral stiffness of the guidance, according to [1]

$$c_{lat} \approx \frac{1}{2} n \cdot c_{long} \quad (11)$$

Here, the number of bars $n = 6$.

The stiffness (c_{long}) is as high as Expression 7 as long as the bar is not deflected. Attention should be given to the fact that an appreciable drop in stiffness occurs as a function of the increasing deflection z . Figure 11 depicts the longitudinal stiffness of a bar ($c_{long} = c_{xx}$) relative to its stiffness at zero deflection (c_{xx0}), as a function of the

relative deflection z/t , with the flexible part q/l as a parameter. In the particular case of $q/l = 1/6$, spring plate thickness $t = 0.6 \text{ mm}$ and amplitude $z = 15 \text{ mm}$ (Figure 10), the longitudinal stiffness drops down to about 20% of that stiffness in the position $z = 0$.

Applied to the number of bars being equal to 6, Expression 11 yields a lateral stiffness as high as $c_{lat} = 12 \cdot 10^6 \text{ N/mm}$ in the zero position in case of the spring plate (Figure 10). In the deflected position the lateral stiffness will drop down to $2.4 \cdot 10^6 \text{ N/mm}$ in this case. The background of Figure 11 is described in the Appendix.

Sensitivity to manufacturing tolerance

We consider the behaviour of the body TB in terms of its radial shift (y , Figure 4) and its tilt (r_y , Figure 4) as a function of the excursion z . As stated before, two spring plates are manufactured on top of each other. We assume that their shapes are identical to a high extent. The result will be that the effective lengths of the flexures T1 and B1 are equal, etc. If the plates are assembled in their relative rotational position, as they were manufactured, tilt errors will be ignorable. As long as the effective lengths l of the flexures 1,2,3 are equal, their virtual retractions p (Figure 7) will be equal:

$$p = \frac{\hat{z}}{2l} \quad (12)$$

The axis of rotation will be the center line through B in Figure 6. However, the lengths of the flexures 1,2,3 may be different. If so, a z -excursion will result in a (parallel) shift of the body in the radial direction (y). Let both the flexures T3 and B3 of Figure 6 have the length $l + e$ rather than l . In the neutral position ($z = 0$) the error e will have no effect. At maximum excursion \hat{z} however, the virtual retraction (Figure 7) of the flexure B3 will be equal to

$$p^* = \frac{\hat{z}^2}{2(l + e)} \quad (13)$$

From Expressions 12 and 13 we derive

$$p_e = p - p^* = \frac{\hat{z}^2}{2} \left(\frac{1}{l} - \frac{1}{l + e} \right) \approx \frac{\hat{z}^2}{2} \frac{e}{l^2}$$

With B1 and B2 remaining unchanged, due to p_e , the body will rotate about the axis parallel to the center line, through P (Figure 6). The radial offset of the center will be estimated as

$$x_{be} \approx \frac{r}{l} \frac{\sqrt{3}}{2} p_e = \frac{1}{\sqrt{3}} \cdot \frac{\sqrt{3}}{2} \cdot \frac{\hat{z}^2 e}{2l^2} = \frac{\hat{z}^2 e}{4r^2}$$

$$x_{be} \approx \frac{15^2}{4 \cdot 100^2} e$$

$$x_{be} \approx 5.6 \cdot 10^{-3} \cdot e$$

Let the spring plates be manufactured at a length error of about 10 μm , then the radial offset will not exceed $x_{be} = 6 \cdot 10^{-2} \mu\text{m}$. We conclude that the linearity, as well as the positional accuracy of the body along the excursion, will be appreciably high.

A last point, in this respect, is to what extent the spring plates are assembled in a centric position in the frame and around the body, respectively. A solution to this problem would be the application of spring nests [1]. Then automatic centering during the assembly operation is achieved. The manufacturing of such a provision at the outer and inner diameters of the spring plates is performed in one manufacturing step with the previously discussed gaps.

Experience

Unfortunately, the development of the linear guidance according to Figure 10 has not been finished up to now. In this respect no reference to practical experience can be made. The reader is invited to apply the described concept and report about his or her experience. ■

REFERENCE

- [1] M.P. Koster, "Constructieprincipes" (Design Principles, in Dutch), ISBN 978-90-5574-610-1, ThiemeMeulenhoff, 2008.

APPENDIX

Longitudinal stiffness of a deflected bar with flexible joints

Procedure

The first step is the determination of the shape of the bar due to small lateral deflections, based on linear theory. The second step is assuming that the shape of the laterally deflected bar in the case of large deflections is directly proportional to its shape as derived from linear theory. As a third step, the curved bar as determined above is the starting point for calculating its longitudinal stiffness, based on linear theory.

As a result, only simple linear theory is applied to determine the longitudinal stiffness of the bar with flex joints, although the lateral deflection is large. In this respect, lateral deflections z are called large if they are large relative to the plate thickness t (see for example Figure 10), where $z = 15 \text{ mm}$ and $t = 0.6 \text{ mm}$.

Lateral deflections

The first step is the description of the shape of lateral deflection. Figures A1a and A1b, respectively, depict halves of the flexure. Next, Figure A1b is rotated about π , yielding Figure A1c. Comparison with Figure A1a yields: $D \neq 0$ and $M = 0$.

The bending moment is derived from Figure A2:

$$M(x) = D(a + q - x)$$

The elastic line

$$\frac{M(x)}{EI} = \frac{d\varphi}{dx}$$

yields the angle of rotation

$$EI \varphi(x) = D(ax + qx - \frac{1}{2}x^2)$$

Because $\varphi(x) = dy/dx$, it is obvious that

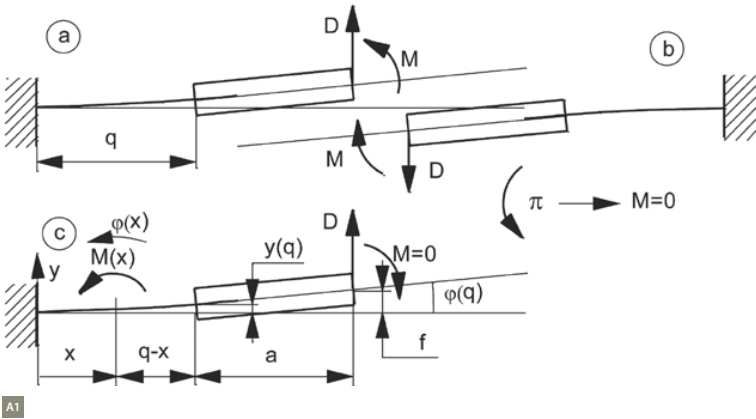
$$EI dy = D(ax + qx - \frac{1}{2}x^2) dx$$

The lateral displacement appears as

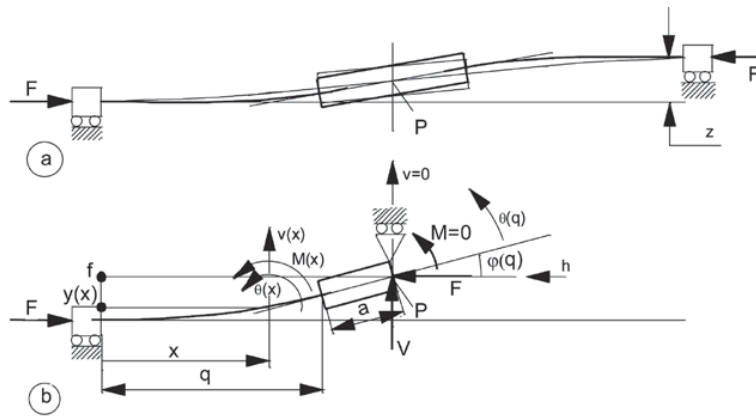
$$EI y(x) = D \left(\frac{ax^2}{2} + \frac{qx^2}{2} - \frac{x^3}{6} \right) \quad (A1)$$

The lateral force D depends on the excursion z . In the center of the bar the offset is $f = z/2$:

$$f = y(q) + a \cdot \varphi(q) \quad (A2)$$



A1



A2

A1 Small, lateral deflection f .

A2 Longitudinal force F and lateral force V on a curved bar.

With the help of Expressions A1 and A2 we arrive at:

$$Elf = D \left(\frac{aq^2}{2} + \frac{q^3}{3} + a^2q + \frac{aq^2}{2} \right)$$

$$D = \left(\frac{Elf}{a^2q + aq^2 + \frac{1}{3}q^3} \right)$$

Introducing $\alpha = a / q$ yields

$$D = \left(\frac{Elf}{\alpha^2 + \alpha + \frac{1}{3}} q^3 \right)$$

Finally, A1 is rewritten as the expression for the shape of small, lateral deflections:

$$y(x) = \frac{f \cdot (\frac{1}{2}ax^2 + \frac{1}{2}qx^2 - \frac{1}{6}x^3)}{(\alpha^2 + \alpha + \frac{1}{3})q^3}$$

Longitudinal deflections

In the second step we take the shape from Expression A5 as representative for *large*, lateral deflections. Next, we apply a load F (Figure A2) on the curved bar. Due to symmetry, applying this load will not affect the location of the center P . The lateral force V maintains this condition.

Applying the elastic line expression

$$El.d\theta = M(x)dx$$

we arrive at an expression for the lateral displacement v at P :

$$v = \int_0^q [q - x + a] d\theta = 0$$

$$Elv = \int_0^q [q - x + a] [V(q + a - x) + F\{f - y(x)\}] dx = 0$$

The shape of the curved bar is known from Expression A5. Performing this integration results in V being directly proportional to F according to

$$\begin{aligned} V &= - \frac{f}{q} \cdot \frac{T}{N^2} \cdot F \\ N &= \alpha^2 + \alpha + \frac{1}{3} \\ T &= \alpha^3 + \frac{4}{3}\alpha^2 + \frac{2}{3}\alpha + \frac{2}{15} \\ a / q &= \alpha \\ f &= y(q) + a \cdot \varphi(q) \end{aligned} \quad (A6)$$

Now we are able to determine the longitudinal deflection of the curved bar (Figure A2) under the longitudinal load F and the lateral load V ; see Expressions A6.

From Figure A2 it can be derived:

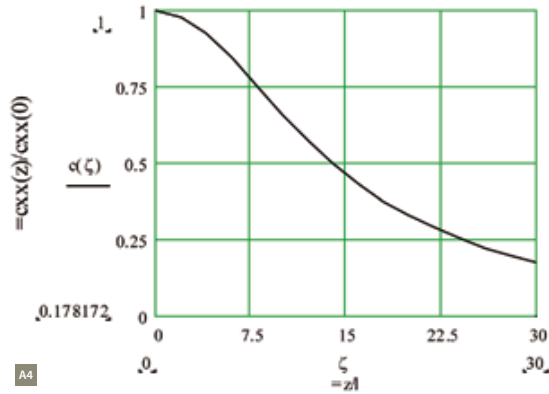
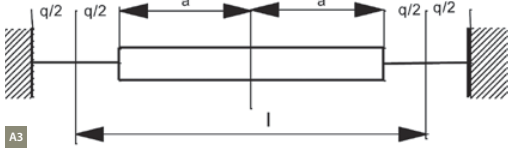
$$M(x) = V(q + a - x) + F\{f - y(x)\}$$

$$\text{Elastic line: } \frac{M(x)}{EI} = \frac{d\theta}{dx}$$

$$dh = \{f - y(x)\} d\theta$$

$$Elh = \int_0^q \{f - y(x)\} M(x) dx \quad (A7)$$

The shape of the bar, $y(x)$, was expressed in A5. The Expression A7 is valid for half of the bar. The result of A7, written in terms of longitudinal compliance



A3 Bar with flex joints.
A4 Longitudinal stiffness of the bar (Figure A3) for the case t (rectangular cross section) and $q/l = 1/6$.

$$\frac{1}{c_{xx}} = \frac{h}{2F}$$

is

$$\frac{1}{c_{xx}} = \frac{z^2 q}{EI} \left[\frac{1}{2N^2} \left[-\frac{T^2}{N} + U \right] \right]$$

$$T = \alpha^3 + \frac{4}{3}\alpha^2 + \frac{2}{3}\alpha + \frac{2}{15}$$

$$N = \alpha^2 + \alpha + \frac{1}{3}$$

$$U = \alpha^4 + \frac{5}{3}\alpha^3 + \frac{17}{15}\alpha^2 + \frac{17}{45}\alpha + \frac{17}{315}$$

$$\alpha = a / q$$

The Expressions A8 only reflect the longitudinal compliance due to bending of the flexures. The longitudinal elongation of the flexures that are not bent should be accounted for as well. The first expression from A8 is extended as follows:

$$\frac{1}{c_{xx}} = \frac{z^2 q}{EI} \left[\frac{1}{2N^2} \left[-\frac{T^2}{N} + U \right] \right] + \frac{2q}{EA} \quad (A9)$$

In case of a rectangular or a circular cross section, respectively, we have

$$I = \frac{b}{12} t^3 = \frac{A t^2}{12}$$

$$I = \frac{\pi}{64} d^4 = \frac{A d^2}{16}$$

Expression A9 is modified as follows:

$$\frac{1}{c_{xx}} = \frac{2q}{EA} \left[\phi_{t,d} \left(\frac{z}{t,d} \right)^2 \frac{1}{2N^2} \left[-\frac{T^2}{N} + U \right] + 1 \right]$$

resulting in the expression for the longitudinal stiffness of the straight bar ($z = 0$) with two flex joints (Figure A3):

$$c_{xx}(0) = \frac{EA}{2q}$$

$$\frac{c_{xx}(z)}{c_{xx}(0)} = \left[\phi_{t,d} \left(\frac{z}{t,d} \right)^2 \frac{1}{2N^2} \left[-\frac{T^2}{N} + U \right] + 1 \right]^{-1} \quad (A8)$$

$$\phi_t = 6$$

$$\phi_d = 8$$

$$T = \alpha^3 + \frac{4}{3}\alpha^2 + \frac{2}{3}\alpha + \frac{2}{15}$$

$$N = \alpha^2 + \alpha + \frac{1}{3}$$

$$U = \alpha^4 + \frac{5}{3}\alpha^3 + \frac{17}{15}\alpha^2 + \frac{17}{45}\alpha + \frac{17}{315}$$

$$\alpha = a / q$$

$$c_{xx}(0) = EA / (2q)$$

(A10)

t: in case of a rectangular cross section
d: in case of a circular cross section

The relationship A10 for the case $q/l = 1/6$ (Figure A3) is depicted in Figure A4. In the section on the lateral stiffness of the linear guidance (Figure 11) characteristics for many q values are drawn. It should be emphasised that these characteristics were derived merely by the help of well-known linear theory. The characteristics closely resemble those by [2] and [3] based on non-linear theory. ■

REFERENCES

- [2] H.M.J.R. Soemers, "Design Principles for precision mechanisms", T-Pointprint, 2011.
- [3] J. van Eijk, "On the Design of Plate Spring Mechanisms", Ph.D. thesis, Delft University of Technology, 1985.

REFLECTIONS ON SELF-ALIGNMENT

A well-known problem in mechatronic systems is how to mount high-precision parts, like masks, lenses, apertures, etc., with high accuracy. Additionally, some applications require component interchangeability, for example for service purposes or mask exchange for the next process step in a deposition tool. For development in the field of EUV lithography, a kinematic mount was designed for an optical component with high stiffness and a repeatability of less than 10 micrometers.

GERRIT VAN DER STRAATEN

Assuming a frictionless contact, a sphere on a flat surface constrains one translation normal to the surface. With three balls in three V-grooves as shown in Figure 1, six degrees of freedom are constrained.

Kinematic mount

With the orientation of the V-grooves a thermal centre (TC) is created in the centre of the kinematic mount. A thermal centre is the point in the module that stays in position during homogeneous expansion of either the optical component or the supporting frame. The advantage is that uniform thermal expansion of the component will not result in a shift of the centre of this component relative to the frame with the V-grooves. The design goal is to create the thermal centre in the most critical part of the component, for example the focus point of a mirror or lens, the centre of an aperture or the centre of a mask.

Lens module

The thermal centre of the kinematic mount of the lens module is placed in the focus point. To that end, the orientation of the V-grooves is changed with respect to the frame. The centerlines through the centres of the spheres and parallel to the V-grooves intersect at the focus point of the lens module.

Stiffness

If the V-grooves are tilted 35° with respect to the base plate, the centerlines of the V-grooves are perpendicular to each other, so the surfaces of the V-grooves are perpendicular to

each other or are in the same plane; see Figure 2. Then the translational stiffnesses in three directions perpendicular to faces of the V-grooves are equal: two times the Hertzian contact stiffness of the sphere on the V-groove's face. To increase the Hertzian contact stiffness, the V-grooves are made as two cylindrical faces with the diameter slightly bigger than the diameter of the spheres; see the detailed view in Figure 3. This is done to create a large contact surface and increase contact stiffness.

Using the HertzWin software [1], the contact stiffness of a sphere on a concave V-groove is estimated: $c_{\text{Hertz}} = 3 \cdot 10^8$ N/m. Now the total translational stiffness can be estimated: $c_{\text{total}} = 6 \cdot 10^8$ N/m.

Coefficient of friction

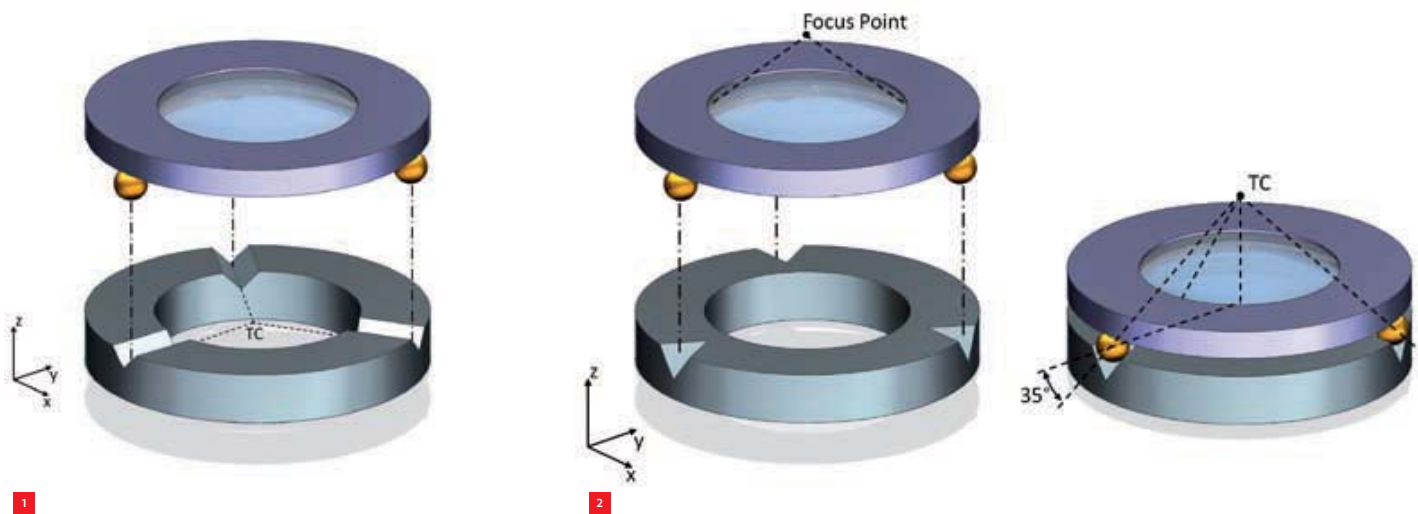
Consider the 2D situation in Figure 4, where a rectangular body is positioned on three hemispheres. The body is positioned correctly if all three hemispheres make contact with the body. Therefore, an alignment force has to be applied to the body such that the friction forces in the two contacts are overcome to enable movement towards the third sphere in any situation.

In any contact point the coefficient of friction can be represented by cones where the coefficient of friction is: $\mu = \tan(\alpha)$. The actual contact force is the sum of the normal force F_n and the local friction force F_f . The working line of this actual contact force is within the angle α . In all 2D contacts this friction angle can be drawn as shown in red in Figure 4.

AUTHOR'S NOTE

Gerrit van der Straaten is a technology consultant and designer at Settels Savenije van Amelsvoort, an engineering consultancy company based in Eindhoven, the Netherlands. This article was, in part, based on a presentation at the DSPE Conference, which was held on 4 and 5 September 2012 in Deurne, the Netherlands.

gerrit.van.der.straaten@stt.nl
www.stt.nl



Consider the situation that the body makes contact with two of the three hemispheres, for example hemispheres 1 and 2 in Figure 4, and for alignment also hemisphere 3 has to be mated. The sum of the moments of the alignment force, the normal forces in contacts 1 and 2, and friction forces in contacts 1 and 2 around the rotation pole P_{12} should result in a rotation of the body towards hemisphere 3. In general, the body will be aligned on three hemispheres if the line of action of the alignment force:

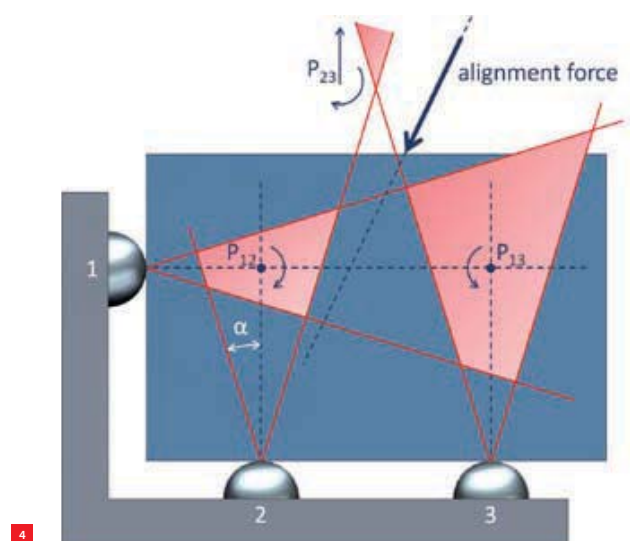
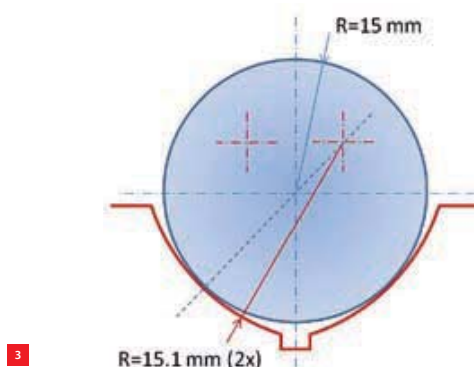
- creates a moment with respect to the three poles (P_{12} , P_{23} and P_{31} in Figure 4) in the appropriate direction for positioning the body on the three spheres;
- does not intersect any region where two friction angles overlap; if the alignment force passes an intersection area it will be decomposed in two support forces and the third support point will not have any preload force.

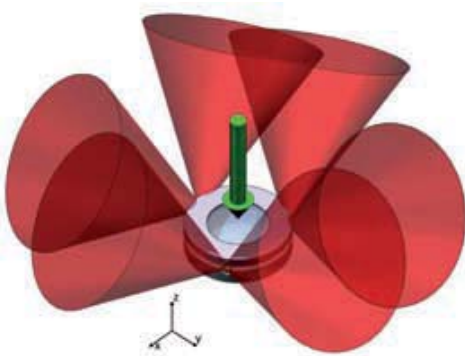
An example of the alignment force that will position the body on the three spheres is drawn in Figure 4. This is a 2D example to determine the alignment force with given

coefficient of friction. This graphical method is applied in 3D to design the V-grooves of the kinematic mount for the optical component.

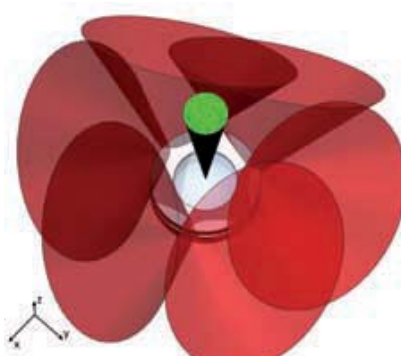
The friction cones are drawn in a 3D CAD model and shown in Figure 5. In this case the coefficient of friction is assumed 0.5, resulting in a half cone angle of 27° . The lens module is aligned by gravity forces. From the CAD model shown in Figure 5 it can be concluded that self-alignment, the situation that the lens module is positioned by gravity forces, is feasible if the coefficient of friction is less than 0.5. Furthermore with a coefficient of friction of 0.5 the total system can be tilted up to 25° around any axis in the XY plane while self-alignment will still take place. If the coefficient of friction is 1, the maximum allowed tilt is about 8° . See Figure 6, where the friction cones are in red and the green cone represents the

- 1 Exploded view of kinematic mount.
- 2 Kinematic mount with tilted V-grooves.
- 3 Detailed view of sphere and V-groove.
- 4 Alignment of 2D body on three hemispheres.

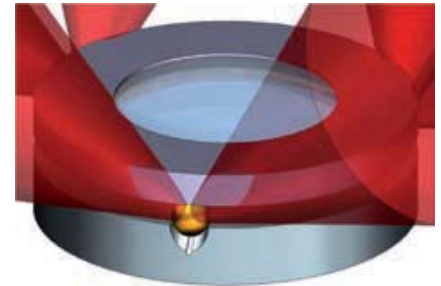




5



6



7

- 5 Friction cones, $\mu = 0.5$.
 6 Friction cones, $\mu = 1$.
 7 Friction cones at V-groove.
 8 Hysteresis measurement.

allowed zone for the alignment force, assuming that the line of action of the alignment force goes through the centre of gravity of the lens module.

Note that at the spheres also two friction cones overlap, so almost every preload force directly on the spheres will lead to self-locking and alignment will not happen; see Figure 7.

Verification

Assuming a coefficient of friction of 0.5, a robust self-aligning V-groove interface could be designed. To verify the assumed coefficient of friction a pin-on-disc measurement was done, with Si_3N_4 spheres on DLC (diamond-like carbon) coated steel plates. The measured coefficient of friction was 0.03-0.05, over a factor of ten lower than the maximum allowed coefficient of friction for self-alignment.

Reproducibility and hysteresis measurements

Repeatability measurements of the V-groove's interface have been performed. A dummy lens module with three reference balls was placed on the V-grooves and the locations of the reference balls were measured on a coordinate measurement machine in x , y and z . The

repeatability of the kinematic mount was better than $6 \mu\text{m}$ in all directions. Also a hysteresis measurement was conducted. The results are shown in Figure 8.

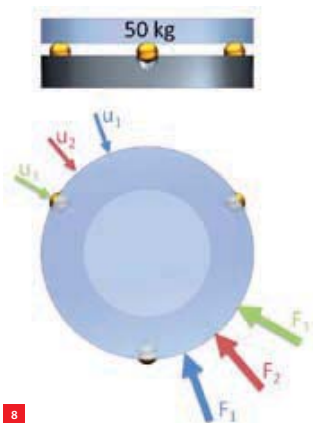
From the results of the hysteresis measurement the total stiffness can be calculated:

$$c = \frac{\Delta F}{\Delta u} = \frac{400 \text{ N}}{6 \cdot 10^{-6} \text{ m}} = 7 \cdot 10^7 \text{ N/m}$$

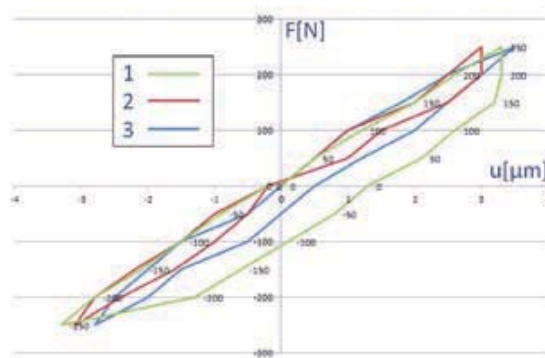
The measured stiffness includes the stiffness of the frames, V-grooves, spheres and Hertzian contact stiffness. The calculated Hertzian contact stiffness of $c = 6 \cdot 10^8 \text{ N/m}$ is in line with the stiffness calculated from the hysteresis measurement.

Conclusion

A design was made for a stiff, repeatable interface for modules like optical components, apertures and masks, where high positioning accuracy is required. To that end, the kinematic mount with three spheres in three V-grooves was modified, resulting in a self-aligning system with high stiffness. ■



8



REFERENCES

- [1] HertzWin, Vink System Design & Analysis, 2009.
 [2] H.M.J.R. Soemers, "Design Principles for precision mechanisms", T-Pointprint, 2011.

RELUCTANCE VS LORENTZ

Ongoing developments in the semiconductor industry lead to conflicting requirements on actuators: a higher positioning accuracy while moving a bigger stage faster for increased throughput. A brief comparative analysis of two types of electromagnetic actuators (Lorentz and reluctance) will be presented, emphasising their specific working principle and their advantages and disadvantages. Some examples and results of internal developments within Philips Innovation Services will be used to support this analysis.

ADRIAN TOMA

If we look to the semiconductor industry today, the chip manufacturers are faced with increasingly tough requirements. On the one hand they desire smaller feature size (Moore's law) and on the other hand the economics is forcing them to ask for increased productivity through higher throughput (higher number of exposed wafers per hour) and/or larger wafer substrate size.

Consequently, the high-precision semiconductor equipment manufacturers will be stranded between not only tough but also conflicting requirements (see Figure 1), achieving a higher positioning accuracy while having to move a bigger (larger mass and footprint) positioning stage faster (with higher acceleration and speed) for increased throughput.

These conflicting requirements are placing a heavy burden on the actuators within the high-precision stages with respect to dissipated power, thermal performance and power electronics. Future developments will be required to sustain these trends. The challenge will be to have very high force predictability (asking for actuators with a highly linear behaviour combined with a high force resolution) in order to satisfy the needed accuracy while providing a significantly higher force density to reduce the strain on the thermal performance and the power electronics roadmap (think for instance of available current-voltage combinations).

Historically, Lorentz actuators have been widely used to achieve the highest accuracy levels. However, the sustained drive for higher force density has made the reluctance actuators a serious alternative despite their shortcomings.

Lorentz actuators

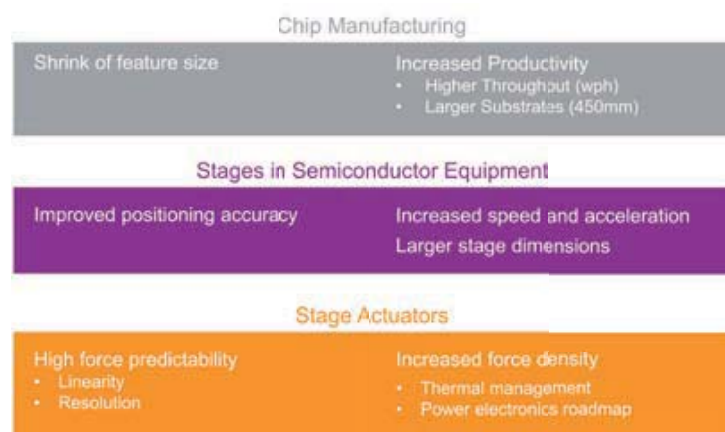
The ideal electromagnetic actuation principle highly desirable from the high-precision perspective is an actuator with a linear relation between force and current, meaning the motor constant should be independent of position, current level, speed, temperature, tolerances and environment (see Figure 2).

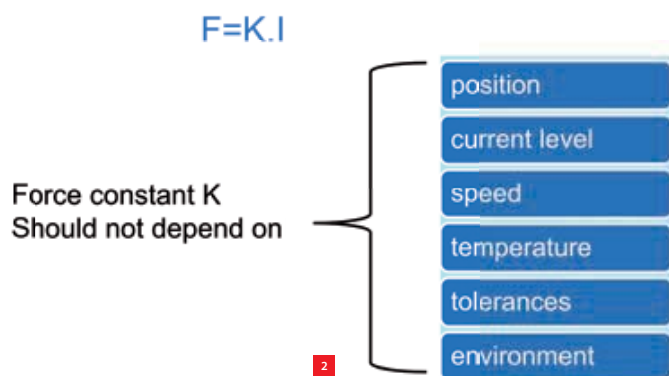
AUTHOR'S NOTE

Adrian Toma is Senior Technologist Electromagnetics at Philips Innovation Services, Eindhoven, the Netherlands. This article was, in part, based on his presentation at the ASPE 2012 Topical Meeting on "Precision Engineering and Mechatronics supporting the Semiconductor Industry".

adrian.toma@philips.com
www.innovationservices.philips.com

1 Challenges of actuators used in high-precision semiconductor equipment stages.





- 2 Ideal actuator from high-precision semiconductor equipment application perspective.
- 3 Lorentz type of actuator.

Lorentz actuators are closest to the ideal, which explains their success within high-precision applications in the past two decades. Their advantages are of course due to their force generation principle. The Lorentz actuation principle is based on force exerted on current-carrying windings situated within a magnetic field. The actuation force can be easily expressed by the following formula:

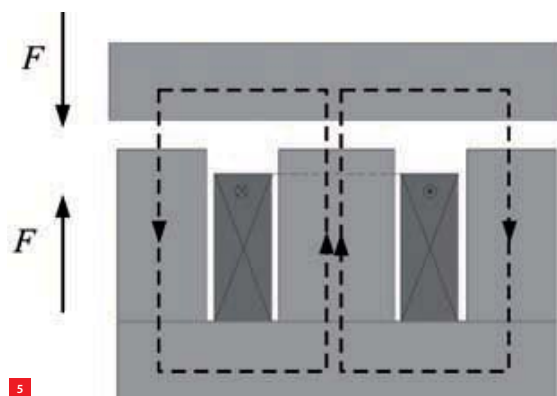
$$\vec{F} = \vec{K}_{\text{linear}} I + \vec{K}_{\text{quadratic}} I^2$$

Here, the force part linear with the current (desirable within high-precision systems) is the dominant part, whereas the force part quadratic with the current is very small, being caused by parasitic effects (a.o. the reluctance effect of the back-iron material behind the permanent magnets, magnetic field non-uniformity, etc.).

One typical example of a Lorentz actuator used for short-stroke stages within high-precision semiconductor equipment is shown in Figure 3; it is composed of coils, permanent magnets and ferromagnetic steel. Within high-precision systems using Lorentz actuators typical values for current density are up to 50 A/mm² and for magnetic field strength up to 0.7 T.

Its advantages for high-precision applications in linearity, easy software implementation and accuracy have prevailed over its drawbacks until now, also because the parasitic effects have been addressed appropriately. In the past decade, significant performance improvements have been achieved both in force density increase as well as in reducing the parasitic effects. These improvements were made possible by incremental innovation in permanent magnets and coil geometry optimisation, development and use of different materials and increasing cooling capabilities.

One example from Philips Innovation Services (PINS) previous experience is reduction of motor constant position

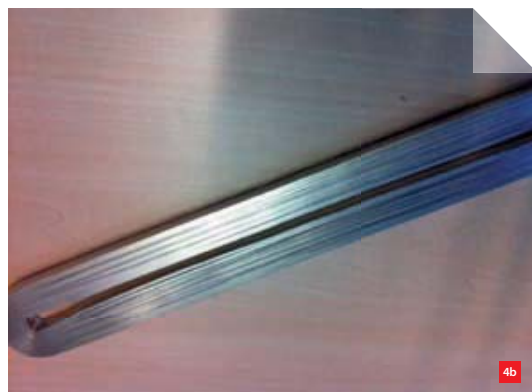


dependency. Lorentz actuators are closest to the ideal actuators, but in fact the motor constant shows minor position dependency and the force also has a current-squared component when displaced perpendicular to the actuation direction, due to the presence of ferromagnetic back-irons. Using our advanced FEM (finite-element model) and analytical modeling tools, we were able to optimise the actuator geometry such that position dependency of the motor constant could be reduced to a minimum. However, as required accuracy within high-precision systems increases even further, small adverse effects (position dependency, damping, tolerances, temperature dependency and stray fields) of this type of actuator will become ever more important.

The major disadvantage of the Lorentz type of actuator is the relatively low force density and steepness, which results in high power dissipation. This weakness combined with the foreseen roadmap of higher accelerations and moving mass will thermally challenge the Lorentz actuators for future high-precision systems.

A more recent development (at PINS) has been the industrially successful introduction of foil coils instead of the classical Cu wires. This introduction has been driven by

- 4 Foil coils.
 (a) Copper.
 (b) Aluminium.
 5 Reluctance type of actuator.



the sustained thirst for higher steepness density for Lorentz actuators in the last period. First steps with Al foil coils were soon followed by Cu foils (see Figure 4) and they proved beneficial, yielding a better thermal conductivity towards the surface where the coil can be cooled; this enabled a higher current density within the coil. Besides, the increased thermal conductivity resulted in an improved temperature uniformity (see Table 1) avoiding undesired hotspots. Another advantage of a foil coil is the superior packing factor due to the rectangular shape of the foil.

An overview of the state-of-the-art values of the performance parameters for Lorentz actuators applied to high-precision systems is given in Table 2.

Reluctance actuators

Despite these achievements, in view of the already discussed challenges in the future the Lorentz actuators will be faced with thermal management issues. So sooner than later we

will need more efficient actuators. A serious candidate is the reluctance actuator. This type of actuator has advantages in steepness density due to the principle of force exerted on a ferromagnetic mover with very high magnetic permeability instead of generating the magnetic field in air where the coil is, as is the case with the Lorentz type of actuator.

The reluctance type of actuation principle is based on attraction force exerted on a ferromagnetic mover by a ferromagnetic armature magnetised by a coil (see schematic of reluctance actuator in Figure 5), which can be described by the following formula:

$$F = C_1 \left(\frac{n \cdot I}{2g + C_2} \right)^2$$

Here n is the number of windings of the coil, I is the coil current, g is the airgap clearance and C_1 and C_2 are constants.

Table 1 Thermal uniformity of aluminium foil coils vs. copper wires.

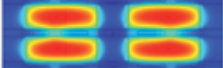

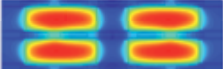
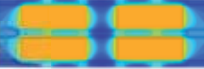
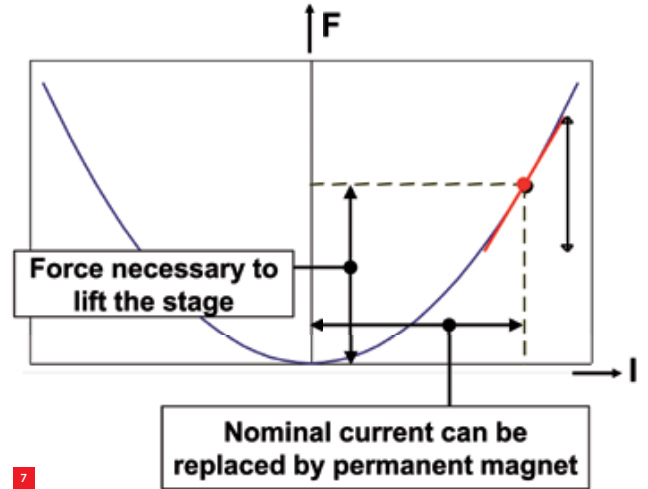
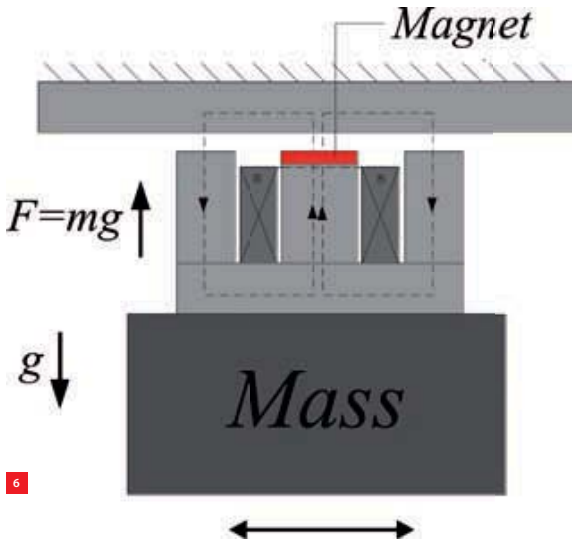
Tmax [°C]	Copper-wire-winded coils	Aluminum-foil-winded coils
Same heat load	 112	 67
Same force (current density)	 112	 92

Table 2 Typical performance parameters for Lorentz and reluctance actuators applied to high-precision systems based on actuators developed within PINS.

Comparative evaluation

Reluctance vs. Lorentz actuators (typical values)

Parameter	Unit	Lorentz	Reluctance
Steepness density	$[\frac{N^2}{W \cdot m^2}]$	$\sim 1e6$	$\sim 8e6$
Position dependency of motor constant	$[\frac{\%}{mm}]$	± 1	± 300
Parasitic stiffness	$[\frac{N}{m}]$	$10 \div 70$	$3000 \div 5000$
Parasitic damping	$[\frac{N \cdot s}{m}]$	$0.1 \div 5$	$25 \div 50$



A brief explanation of the principle: The coil magnetises the armature, which attracts the ferromagnetic mover in order to minimise the magnetic resistance along the field path. Obvious disadvantage is of course the nonlinear relation between the force and the gap on one hand and between the force and the current in the coil on the other hand. Another shortcoming of this basic topology is that only an attracting force can be generated, whereas any self-respecting high-precision application attempting dynamic position control will need bidirectional force generation.

This dilemma can be solved in a most straightforward way for actuation perpendicular to the gravity direction by placing two reluctance actuators back to back, but for actuation in gravity direction a more elegant solution can be found by adding a permanent magnet which pre-stresses the armature towards the mover (see Figure 6). In this way, gravity compensation will be integrated with the vertical actuation in the same actuation module.

The static force of the permanent magnet attracting the ferromagnetic mover will create an offset force at zero current enabling bidirectional force generation around this point, which we did not have when no magnet was present. In this configuration the generated force can be described by the formula:

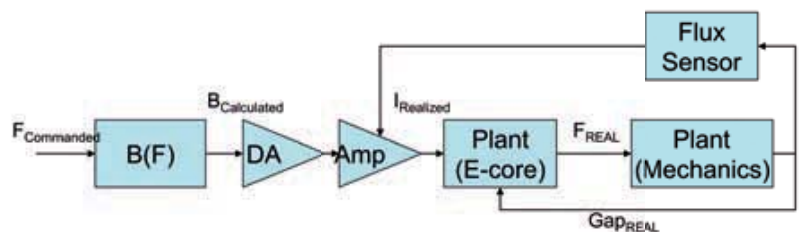
$$F = C_1 \left(\frac{h_m H_c + n \cdot I}{2g + C_2} \right)^2$$

Here n is the number of windings of the coil, I is the coil current, g is the airgap clearance, $h_m H_c$ is the field strength of the magnet and C_1 and C_2 are constants. Consequently, a force offset is introduced which enables bidirectional actuation (see Figure 7).

The nonlinear force-current and force-gap relations, the negative stiffness and the high force variation are the major reasons why the reluctance type of actuators has not been implemented in the past in high-precision systems. Previous publications have highlighted these shortcomings. However, a recent example of reluctance actuators applied successfully within semiconductor stages is the rotary REBL maglev stage, which PINS developed for/together with KLA-Tencor (see Figure 8).

6 Bidirectional reluctance type of actuator combined with gravity compensation.

7 Bidirectional actuation enabled by permanent magnet gravity compensation within a reluctance actuator.





8 Rotary magnetic levitation stage for KLA prototype REBL e-beam writer using bidirectional reluctance actuators (radial actuator in the left inset, vertical actuator in the right inset) enabled by permanent magnet gravity compensation.

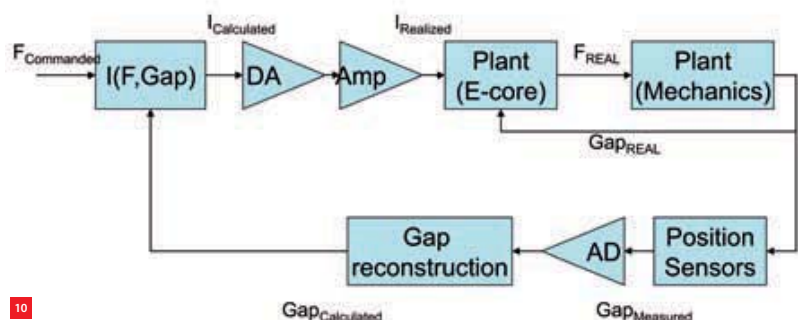
9 Flux control diagram of a reluctance actuator.

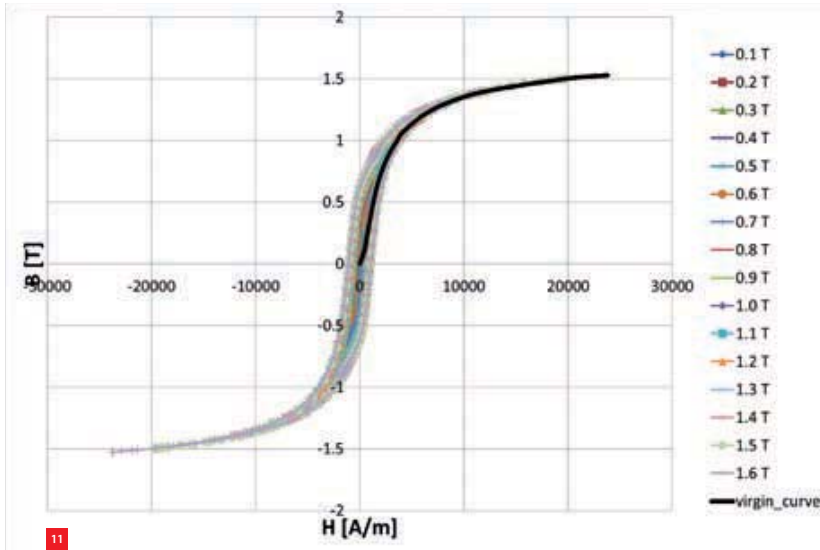
10 Current control diagram of a reluctance actuator.

Both horizontal and vertical active magnetic bearings are provided with reluctance actuators enjoying their advantages on high steepness and low power dissipation. The vertical reluctance actuator is equipped with a permanent magnet as described previously in order to compensate for the gravity and enable the bidirectional force control. This application example has clearly valued more the reluctance type of actuation advantages like high force density, high steepness and low power dissipation against the disadvantages. This is also due to the fact that appropriate measures were taken to compensate for the inherent adverse effects of the reluctance actuators.

Due to their nonlinearity, one important aspect to be taken care of when applying reluctance actuators within high-precision systems is how to address the actuator control. Traditionally, there are two methods of controlling the reluctance actuator. One option is to use flux control (see Figure 9), which makes the force gap-independent. In our implementation we integrated a Hall sensor element into the armature to measure the flux and feed it back to the amplifier. This is a simple method, which requires little software compensation effort, but it has the drawback of analogue calibrations and the final negative stiffness reduction is only 80% (due to implicit limited accuracy of flux measurement in our implementation). In our configuration with only one Hall sensor, sensor performance was the limiting factor.

A second, more effective option is to use current control (see Figure 10), which however makes the force strongly gap-dependent. This can be compensated for by using a sensor to measure the airgap. This method reduces the negative stiffness significantly (by 99%). On the other hand, it requires more complicated software compensation effort as all the implemented calibrations are made in software. Once the calibration procedure software is available, it can turn into an advantage as higher flexibility with respect to change management can be achieved when using software rather than analogue settings.





11 Measured hysteresis curves of ferromagnetic material.

A specific disadvantage of the reluctance actuators (which will become more and more important in view of the future challenges) is the force-displacement hysteresis behaviour caused by the hysteresis intrinsic to the ferromagnetic materials that are used for the armatures (see Figure 11). Clearly, if the material is first magnetised and then demagnetised it will not return to exactly the same working point. Moreover, the impact of this effect on the performance becomes even larger as there is usually a spread in the quality of the ferromagnetic material properties due to the manufacturing process and the thermal treatments applied to the material. Tighter tolerances on the material quality might be needed in the future.

Due to the fact that the reluctance actuators are utilising ferromagnetic materials for force generation both in the moving and the stationary part, if not carefully designed, large damping forces can occur in the actuator. In recent applications, novel laminated-steel topologies were implemented where eddy currents were minimised within the actuator, while for reluctance actuators with complex topologies, unconventional powdered-iron materials can be used for reducing damping forces. An overview of the state-of-the-art values of the performance parameters for

the reluctance actuators applied to high-precision systems is given in Table 2.

Towards future requirements

The actuators used in high-precision applications have come a long way and have changed status from basic building blocks and simple electromotors to become full mechatronic system components playing their part (together with the rest of the system) in achieving accuracy by being robust against disturbances and having a highly predictable behaviour.

Comparing the two actuator types' state-of-the-art against a set of criteria (performance parameters relevant within high-precision semiconductor equipment; see Table 2) learns that reluctance actuators score better than their Lorentz counterparts on steepness density, which is higher by an order of magnitude indicating better performance in force density and power dissipation.

It is also the only winning parameter as nothing comes for free and this advantage comes at a significant cost in adverse effects such as parasitic stiffness and damping and actuator sensitivity to tolerances and movements. The latter strongly underlines the care and attention that have to be paid at actuator level as well as at system level when applying these actuators in high-precision positioning systems. Force predictability has to be very high within high-precision applications. Very small adverse effects may be either tolerated (Lorentz actuators) or they should be compensated for very well (reluctance actuators). Careful judgment in selecting the performance-relevant effects to be compensated for and in deciding upon the implementation method of these compensations in software, is required.

To meet future requirements, Lorentz actuator developments should address thermal management improvements by e.g. applying different coil topologies, novel forcer build-up and innovative cooling strategies. On the other hand, reluctance actuators should build upon further developments in advanced control strategies (benefiting from developments in computing power and software flexibility), accurate sensing systems and new armature designs. ■

Miniature Drive Systems for Aerospace and Aviation

- DC-Micromotors
- Brushless DC-Motors
- Linear DC-Servomotors
- Stepper Motors
- Piezomotors
- Ball Screws
- Precision Gearheads
- Motion Control
- Encoders

WE CREATE MOTION



FAULHABER

MINIMOTOR Benelux · www.faulhaber.com

CONSTRUCTOR AWARD FOR STEFAN SPANJER'S ROBOT HAND DESIGN

At the Precision Fair 2012 in Veldhoven, the Netherlands, the Wim van der Hoek Award was handed out once more under the auspices of DSPE. The award was given to Stefan Spanjer, whose University of Twente graduation project was a robot hand design. The jury commended the simplicity of his design along with the excellent arithmetic execution.



■ Award name giver Wim van der Hoek (second from the left), award winner Stefan Spanjer (fourth from the left), and jury members Marc Vermeulen, Hans Steijaert, Jos Gunsing, Piet van Rens and Wouter Vogelesang (from left to right).

The Wim van der Hoek Award – also called the Constructor Award – was introduced in 2006 to celebrate the 80th birthday of the grandmaster in design principles, Wim van der Hoek. From 1962 to 1985, while working at Eindhoven University of Technology, he laid the foundations for the unique Dutch method of designing mechanical constructions. The Constructor Award is presented annually for the best graduation project in the field of mechanical engineering construction at the three universities of technology. This award includes a certificate, a trophy made by the Leiden Instrument Makers School and a cash prize of €1,000, sponsored by the 3TU Centre of Competence High Tech Systems. The jury comprises representatives from industry, education and applied research. Jos Gunsing is the jury chairman on behalf of the DSPE board. He is a technology innovator at MaromeTech in Nijmegen and Mechatronics lecturer at the Avans University of Applied Sciences in Breda.

Playing with degrees of freedom

This year the award went to Stefan Spanjer for his Master's thesis, "Improved Grasp Robustness Through Variable Transmission Ratios In Underactuated Fingers". He graduated in Mechanical Engineering Automation and Mechatronics from the University of Twente under the supervision of Prof. Just Herder of

the faculty of Engineering Technology. His thesis was a design for a robot hand, in particular the finger controls. Improving gripping skills is one of the biggest challenges for robot designers. The judges were especially taken with the simplicity of Stefan Spanjer's design and his excellent mathematical execution. "What was refreshing was the way

he played with the degrees of freedom and was able to combine the power and position controls in a compact hand." On Thursday, 29 November, Stefan Spanjer was presented with the award by jury chairman Jos Gunsing, in the presence of Wim van der Hoek, after whom the award was named. ■

Ten free Mikroniek subscriptions

At the DSPE stand on the Precision Fair 2012, there was a raffle for ten free, one-year Mikroniek subscriptions. The winners are:

- Mr. M. Algra, VDL ETG, Almelo
- Mr. J. Bos, Velddriel
- Mrs. K. Damstra, YER, Den Haag
- Mr. F.S. de Graaf, Norma IMS, Drachten
- Mr. M. Kasbergen, Schoonhoven
- Mr. H. Kik, Rotterdam
- Mr. W. Maan, CERN, Grenoble
- Mr. M. Mishra, NXP Semiconductors, Nijmegen
- Mr. T. Scheerder, VDL ETG, Eindhoven
- Mr. E. Smit, Timskire Holding, Nieuwegein

In memoriam George van Drunen

George van Drunen passed away on 17 January 2013. His spirit was strong, but his body could not go on. George served as secretary to DSPE in the 80s and 90s and was of great service to our association. In the years that followed, he kept track of DPSE with interest, also advising me as chair. We spoke to each other by phone a few times a year and he was always kindly disposed towards DPSE. We would like to thank George for everything. May he rest in peace. Our sincerest condolences go out to his partner Joke and his sons.

Hans Krikhaar
President DSPE

MORE MAKING AND MEASURING

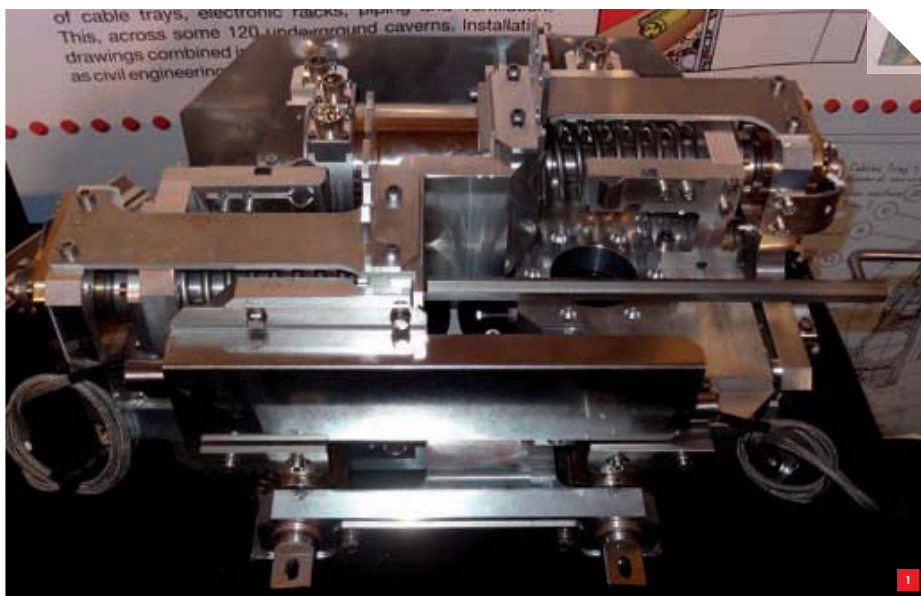
With more exhibitors (260) and visitors (nearly 3,600), the Precision Fair 2012, organised by Mikrocentrum on 28 and 29 November in Veldhoven, the Netherlands, was larger than ever. The fair showed much more manufacturing and measuring stands than ever before. And many metal machining specialists showed their ambition to enlarge their cutting and grinding activities with disciplines like assembly, drive and control, for the delivery of complete functional units.

FRANS ZUURVEEN

Countries at the other end of the world, with China as the most prominent one, are more and more being regarded as the world's manufacturing regions. But this Precision Fair demonstrated that companies in our country and neighbouring Germany are indispensable when dealing with real precision in the submicron or even nanometer area, even more so with the application of exotic materials. Lectures by CERN representatives and demonstrations of precision assemblies showed real evidence of this (see Figure 1).

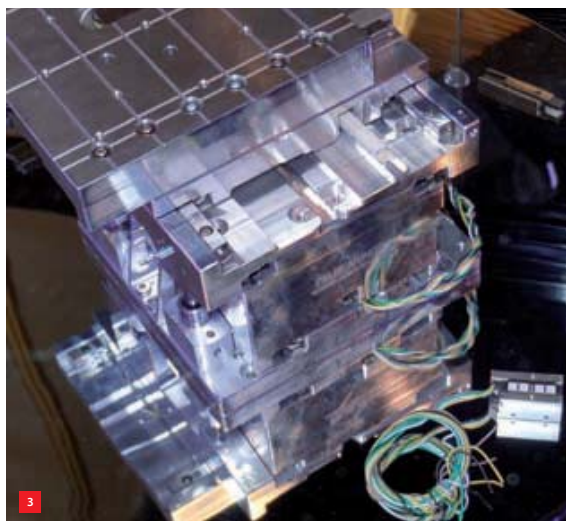
Technology Hotspot

In the Technology Hotspot, students from various educational institutes seized the opportunity to demonstrate challenging examples of the application of precision mechanics. They made evident that young people are not reluctant to opt for an exact field of study. Prominent was the stand of 3TU, the three Dutch universities of technology: Delft, Eindhoven and Twente. Some universities of applied sciences were also present, as was LiS, the famous Leiden Instrument Makers School.



AUTHOR'S NOTE

Frans Zuurveen is a freelance text writer who lives in Vlissingen, the Netherlands.



- 1 A motorised positioning table for a beam collimator, made by the European precision industry for CERN, the European Organisation for Nuclear Research.
- 2 The first Femtoprinter. The inset shows a micro-displacement sensor on a glass substrate realised with this instrument. (Photos courtesy of TU Eindhoven)
- 3 A precision 3D stage designed and manufactured by PM-Bearings. It realises controlled 1 nm steps thanks to piezo-electric drives from PiezoMotor.
- 4 A burner housing made by MTSA Technopower.
- 5 An aluminium test piece for a pulse compressor for SwissFEL, made by VDL ETG.

Very interesting was the Femtoprint project by a European team including TU Eindhoven (see Figure 2). The term femto (10^{-15}) does not refer to dimension but to time: a pulsed femtosecond laser is being applied. The goal is to provide users with the instrumentation and technology to produce their own microsystems. Areas of application include biotechnology, optical memories, polymer micro-moulding, sensors and actuators, lab-on-a-chip and a variety of optical components. The basic two-step process combines laser exposure of a light-sensitive resin on a glass substrate with chemical etching.

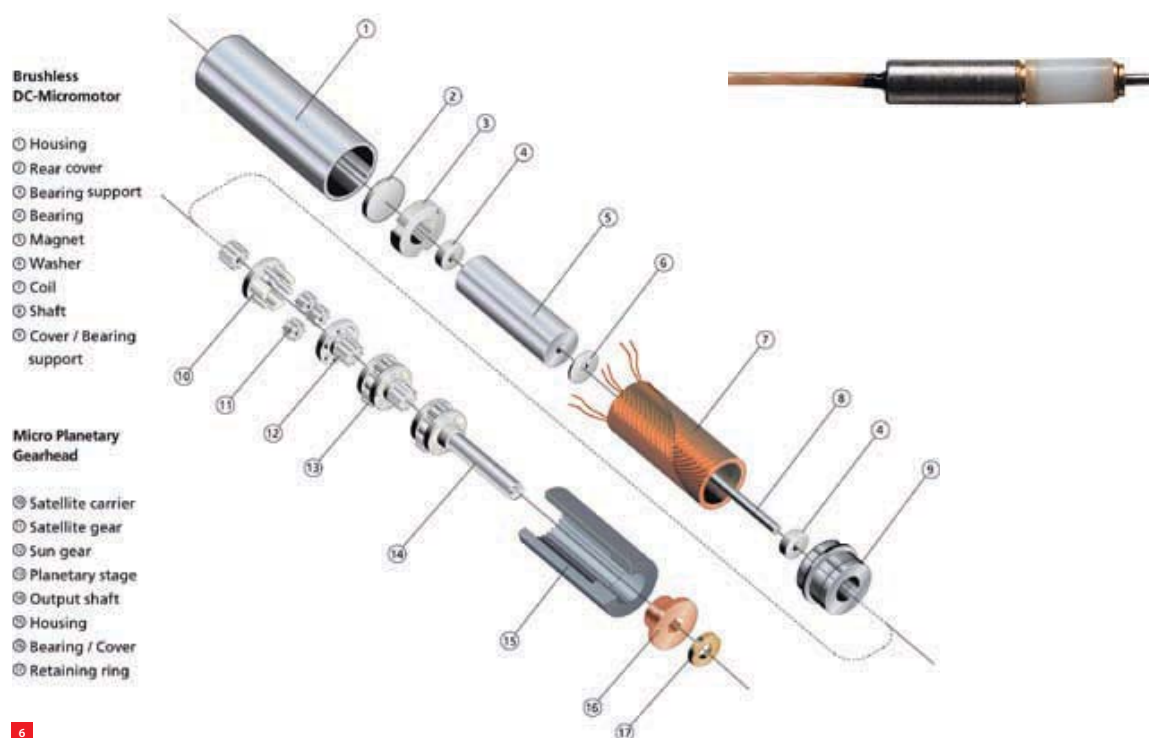
Precision units

A clear example of precision part manufacturing combined with drive, measurement and control was a 3D stage made by PM-Bearings in Dedemsvaart (see Figure 3). PM-Bearings cooperates with PiezoMotor in Sweden, which manufactures miniature piezo-electric drives for steps down to only 1 nm. For motion control Renishaw metal measuring scales feedback table positions. Negative play between precision-

manufactured slide components results in a continuous pre-tension without the application of springs.

Another firm delivering complete functional units is MTSA Technopower in Arnhem, which covers the entire process from design to manufacturing and service. MTSA is a continuation of the development department of Shell Research Arnhem. It not only disposes of advanced metal machining equipment including spark erosion, but also has a clean room for dust-free assembly. At the fair, they showed a cooling flange for the IC industry and a burner housing (see Figure 4).

Comparable in some aspects is VDL ETG, a continuation of the former Philips Machinefabrieken. They make complete assemblies too, for example for SwissFEL, a free-electron X-ray laser currently being built at the Paul Scherrer Institute in Switzerland. At the fair, VDL ETG showed a large test piece in aluminium with an accuracy of $5 \mu\text{m}$ (see Figure 5), for a pulse compressor in this project.



6

Extremes in driving and positioning

PiezoMotor belongs to the Faulhaber Group, dating back to 1958, when Fritz Faulhaber invented an electric motor with ironless rotor. A real precision product of Minimotor, also belonging to the Faulhaber Group, is the world's smallest brushless DC motor, with a diameter of 1.9 mm (see Figure 6). A miniature planetary gearbox reduces its rotational speed of $100,000 \text{ min}^{-1}$.

The high-performance synchronous motors of IDAM, belonging to the Schaeffler Group, are positioned at the other dimensional end (see Figure 7). These multipole motors with high torque – up to 215 Nm – are available with internal or external rotor with permanent magnets. IDAM's delivery programme also includes ironless linear motors with printed-circuit moving coils.

CCM in Nuenen also designs innovative precision assemblies, from idea to realisation, without having real machining facilities on its premises. CCM showed an application of a steel conveyor belt in a colour inkjet printer (see Figure 8), in which successive prints have to match very accurately. Therefore, the belt has to move with extreme precision. To control the sideways movement, the belt is provided with a narrow track, which is being monitored by a sensor. Longitudinal control is accomplished by integrating angle encoders in the driving rollers. The various arrangements result in an overall accuracy of $10 \text{ }\mu\text{m}$.

Making precision parts

A special technological discipline is machining granite for precision machinery and measuring rooms. Represented at the fair was Mytri from Apeldoorn, which for more than seventy years has been a supplier of base frames, surface plates, etc., from extremely stable natural stone. Accuracies of $1 \text{ }\mu\text{m}$ per 1,000 mm length are attainable thanks to scrupulous handwork. Mytri also supplies cast-iron precision flatness products.

Figure 9 shows examples of products manufactured from solid metal by conventional metalworking, i.e. removing material. Nowadays, products can also be realised by building them up in layers: additive manufacturing. This technology used to be limited to non-metallic materials, but LayerWise in Leuven, Belgium, succeeded in applying additive manufacturing to metals, including alloys that are very hard to machine. Figure 10 shows a complicated LayerWise product.

Measuring precision parts

Just like precision engineers in the last century used to speak straightforwardly about microns, their contemporary colleagues speak with the same ease about nanometers. Nowadays resolutions of measuring systems seem to nearly reach atomic-scale dimensions. But words mean less than facts and resolution is not equivalent to accuracy. So, accuracy statements should not be taken merely on trust.

6 Exploded view of the world's smallest brushless DC motor (see top right), with a diameter of 1.9 mm, a product of the Faulhaber Group. (Photos courtesy of Faulhaber)



Hexagon in Waalre showed the large Leitz Infinity 3D coordinate measuring machine with a large measuring volume of 1,200 x 1,000 x 700 mm³ (see Figure 11). With a guaranteed accuracy of $\pm 0.3 + L/1,000 \mu\text{m}$ (L in mm), the overall accuracy is $\pm 1.3 \mu\text{m}$ for the complete measuring range. All slides are supported by air bearings and systematic errors have been software-compensated. Remarkable is the (X,Y)-movement of the measuring table with a – very stable – stationary portal for the Z-axis. This is unlike the usual set-up with the Y-axis moving along the horizontal beam of the portal, which moves in the X-direction, as for example in the Mitutoyo Quick Vision Apex.

Leitz applies Heidenhain optical measuring scales, whereas Mitutoyo uses its own scales, developed in-house from crystallised glass with a resolution of 20 nm. In its stand, Heidenhain Nederland presented optical scales with the highest precision, alongside their scales with the lowest

price. The newly developed scales LIP 200 on Zerodur (Schott glass ceramic with extremely low thermal expansion) have a pitch of 512 nm and a deviation within one period of only $\pm 1 \text{ nm}$. Heidenhain claims a positional noise of 0.150 nm RMS for these scales. The LIDA 200 scale is relatively cheap and has a pitch of 200 μm . Both scales measure incrementally and are available up to a maximum length of 3 m.

As at previous fairs, FARO Benelux showed its measuring arms with angle encoders in three hinges. Their accuracy of about 40 μm is rather limited but is guaranteed within a large half-sphere with a radius of 1.35 m. The advantage of such measuring systems is their ease of use.

Measuring with a glass fibre stylus on a Werth Scope-Check CMM may be considered as the other end of the accuracy range. The fibre stylus has a smallest ball tip diameter of only 20 μm and is part of the Werth Multisensor system, in

- 7 High-performance synchronous motors by IDAM with internal or external rotor with permanent magnets.
- 8 A position-controlled steel conveyor belt for an inkjet colour printer, designed by CCM.
- 9 High-tech products from solid metal.
(a) A leaf-spring parallel guidance made from solid steel by Norma.
(b) A turbine rotor made from solid aluminium by Aalberts Industries, a conglomerate of companies for industrial products, systems and processes.



10



11



13

10 A metal model of the Brussels-based Atomium, resembling the cubic atomic structure of iron, made by LayerWise using additive manufacturing.

11 The Leitz Infinity 3D coordinate measuring machine with a large measuring volume of 1,200 x 1,000 x 700 mm³.

13 The Qioptiq mag.x System125 micro-inspection system.

which many kinds of styli are applicable for measuring one workpiece in a single clamping. One of the advantages of the optical-sensor monitored fibre stylus is the low touching force of as little as 1 μ N. This is in contrast to conventional steel styli, which have to work with stiff stylus arms, with a relatively high touching force as a consequence.

Renishaw was, of course, also present at the Precision Fair, showing its linear encoder with a resolution of 1 nm (see Figure 12). The optical-scale pitch is 20 μ m and the accuracy amounts to $\pm 1 \mu$ m at a measuring length of 1,000 mm. Two versions are available: incremental and absolute.

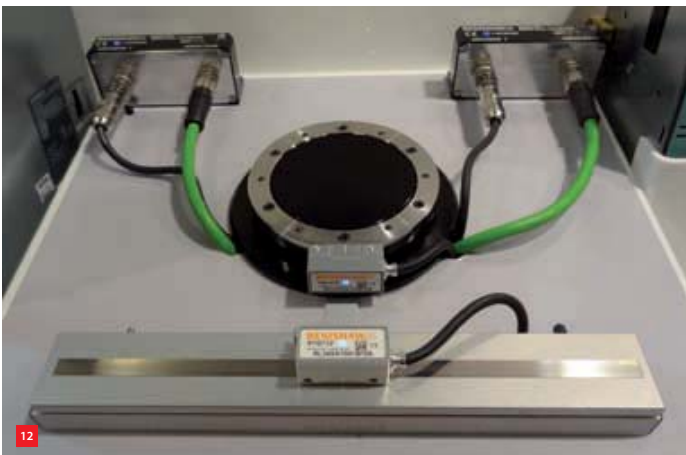
12 A Renishaw linear optical encoder (below) with a resolution of 1 nm and an accuracy of $\pm 1 \mu$ m per 1,000 mm. Above an angular encoder.

Vision with precision

Qioptiq is a German optical company with its head office in Feldkirchen, which combines the disciplines of various firms, including famous names like LINOS, Rodenstock and

Spindler & Hoyer. Qioptiq not only manufactures sophisticated objective lens components but also complete optical systems. At the fair, Qioptiq showed the variable mag.x System125 micro-inspection system (see Figure 13). The system uses high-resolution large-format detectors and sensitive line-scan sensors to inspect large areas at high speed. Thanks to the application of a telecentric beam path, the system can also perform measurement tasks. The objective has a large numerical aperture for a high resolution in visible light.

Still higher resolutions are attainable when working with electrons in a scanning electron microscope (SEM). But users are reluctant to work with SEMs because of their high price and a slight antipathy towards vacuum ("horror vacui"). PhenomWorld in Eindhoven, in which FEI, NTS and Sioux participate, delivers the user-friendly Phenom, a combination of an optical microscope and SEM, for less than 50,000 euros. Visible light is used for easy inspection and path finding at low magnification, while the electrons enable much larger magnifications – up to 45,000x – for detailed observations. ■



12

INFORMATION

WWW.PRECISIEBEURS.NL

ALM PARTS IN SPACE

In collaboration with the European Space Agency (ESA), LayerWise produced injectors, combustion chambers and expansion nozzles representative of a bi-propellant communication satellite engine through Additive Layered Manufacturing (ALM). These parts enable ESA to assess ALM's potential to further improve the manufacture of current designs. In addition, ESA and LayerWise specialists exploited ALM's design opportunities to engineer functionally separated design alternatives.

AUTHOR'S NOTE

Rob Snoeijls held several R&D, marketing and services positions in technology firms in the USA, Belgium and the Netherlands, and now is a marketing manager for Belgian company LayerWise.

rob.snoeijls@layerwise.com

ROB SNOEIJS

With Additive Layered Manufacturing, LayerWise saves weight, simplifies assembly, speeds manufacturing, and supports late-stage design adaptation. The collaboration with the European Space Agency fits in LayerWise's strategy to offer its unique ALM know-how in support of space and aerospace manufacturing excellence.

The current state of ALM

Communication satellites are essential for mobile internet and secured financial communication between banks, direct TV broadcasting, and earth observation for weather forecasting. One of ESA's roles is to oversee development of in-space satellite engine technologies. As part of an internally funded program ESA is investigating the current

state of metal Additive Layered Manufacturing, assessing its potential and maturity in light of future engine developments.

As part of the research programme, ESA selected LayerWise because of this company's ALM technology expertise and customer services offered. LayerWise produced the current designs of three critical engine parts, as well as alternative ALM-enabled functional design variants.

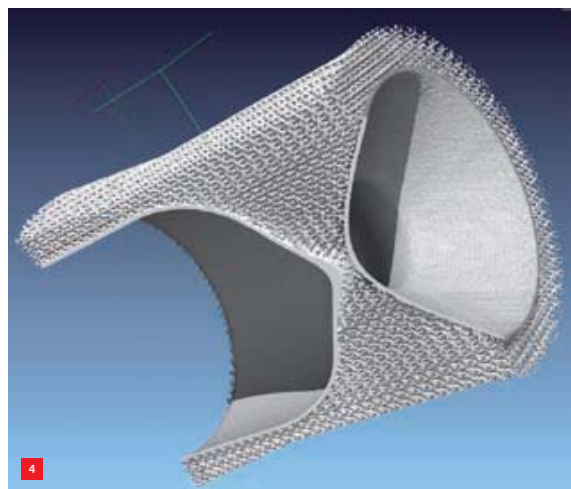
The injector part of a satellite engine brings two propellants together in a controlled way, igniting spontaneously and burning continuously. The venturi-shaped combustion chamber accelerates the chemical exhaust gases to power the satellite to the right orbit. The expansion nozzle impacts the motion characteristics by influencing the gas flow further downstream.

1 Injector design is a compromise between propellant's flow conditioning and thermal isolation. Innovative ALM manifolding allows optimised propellant's flow from the valve to the combustion chamber.

2 Judging from X-ray images with 130 micron resolution, ALM is a practicable approach to injector manufacturing.



- 3 Separating combustion chamber functions between operational and non-operational load cases, translates into strut-work ribs supporting the thin wall.
- 4 A promising design opportunity resulted in an ALM low-density mesh on the radiating surface supporting the thin wall of the engine combustion chamber.



Innovative injector manifolding

“ALM offers innovative manifolding to optimise the flow from the propellant valve to the combustion chamber”, says ESA’s propulsion engineering specialist, Simon Hyde; see Figure 1. ALM’s design freedom enables ESA to reduce the number of injector assembly parts to one, coming from more than five with conventional manufacturing; eliminating many risky sealing welds required to achieve reliable hydraulic injection operation; reducing cost and risk considerably. By acquiring full control over the ALM production process, LayerWise achieves a homogeneous microstructure with a relative density of up to 99,98%, for an increasing number of metals and alloys including titanium; see Figure 2.

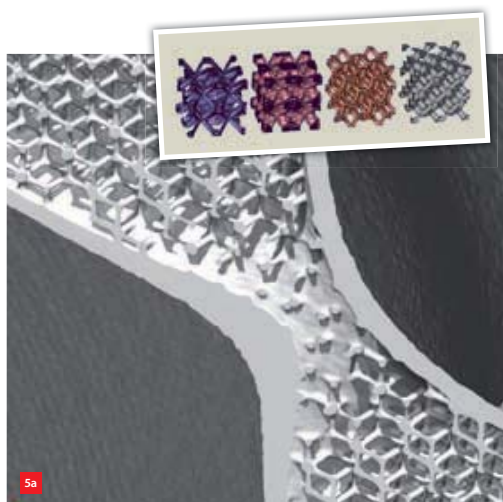
ALM is also suitable for establishing an injector thermal design that prevents heat from soaking back to the sensitive propellant valve’s seat and the spacecraft itself. The absence

of tooling access constraints allows the redesign of the thermal stand-off by controlling the conductivity using a metal scaffold instead. Built in a flight-capable titanium material (Ti6Al4V), the injector parts are approaching the product assurance requirements of the space sector and the design needs of the rocket motor designer.

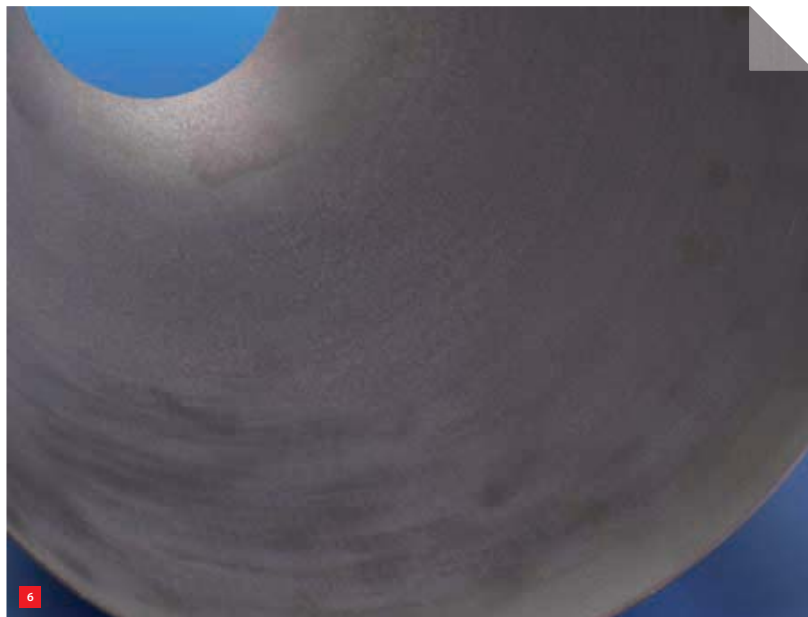
Separated chamber functions

The combustion chambers of compact in-space satellite engines typically consist of a convergent/divergent nozzle with an unsupported nozzle exit. The propellant reactions complete in the convergent section before the exhaust gases flow through the throat contraction into the divergent section where they are expanded supersonically. Existing chambers are designed to withstand the non-operational loads associated with the launch, with thicker walls reacting these transient loads. Once on station and operational, the chambers do not need such thick walls.

- 5 Low-density meshes by ALM.
- (a) The ability to build low-density meshes by using ALM has become a standard feature in ALM software.
- (b) Producing scaffolding meshes would be difficult to realise traditionally, but is comparatively simple for ALM.
- (c) The ALM mesh with 12% volumetric density allows for major combustion chamber weight reduction.



6 The expansion nozzle with an exit diameter close to 50 centimeters is probably the largest ALM part ever built.



ALM allowed the chamber functions to be separated between operational and non-operational load cases. Intuitively, this translates into strut-work ribs supporting the thin combustor wall and the weld flange for the attachment of the expansion nozzle; see Figure 3. Instead of the crude strut work, LayerWise produced the support structure as an ALM low-density mesh; see Figure 4. As its volumetric density is as low as 12%, ALM potentially yields major combustion chamber weight reduction or improvement of the structural safety margins; see Figure 5.

Built in Ti6Al4V material, the true chamber material would be a refractory material alloy (e.g. based on niobium, molybdenum, tantalum, tungsten, and/or rhenium) to withstand the extreme combustion heat. Further investigation of this revolutionary combustion chamber design involves the study of the mesh's isotropy in the stress field as well as its detailed thermal impact. This mesh will increase the effective surface emissivity, so it will certainly influence the heat fluxes around the chamber.

Large-scale ALM

ESA engineers also examined ALM for manufacturing an expansion nozzle with an exit diameter close to 50 centimeters; see Figure 6. This is probably the largest ALM part ever built. Talking about ALM production volume, LayerWise is able to produce any part geometry that fits in a 275 x 275 x 450 cubic millimeter box. The stress in the nozzle is comparatively low and minimising the overhung mass is critical for increased margin on the cantilever engine design. LayerWise produced the ALM expansion nozzle in titanium (Ti6Al4V), which largely meets the mechanical and thermal requirements for the expansion nozzle.

Quality inspection

Visual inspection of the various ALM parts showed that there were no immediate flaws in the mesh or visible pores on any of the surfaces. CMM and X-ray inspection showed that critical features were within 0.1 to 0.25 mm of the nominal design (dimensions and location). Mounting flanges had a flatness of 0.01 mm. Wall thickness was measured at 1.3 mm with a resolution of 130 micron.

According to ESA's Simon Hyde, ALM offers distinct fabrication advantages compared to traditional spin forming of sheet material that kills all design flexibility. ALM allows the engine performance to be tuned towards customer-specific thrust profiles, leaving many design options open until late in the process. ■

INFORMATION

WWW.LAYERWISE.COM
WWW.ESA.INT

Ball Screws

WE CREATE MOTION



- Miniature DC-Motors
- Miniature BL-Motors

FAULHABER

MINIMOTOR Benelux · www.faulhaber.com

THROUGH THE WALL

High-precision machines often require a high vacuum level. Contamination due to moving cables and bearings of the positioning stages within is an issue, which can be solved using an inverted planar motor [1]. However, this solution leads to a complex system due to position-dependent commutation and a large number of coils. An alternative stage design was made at MI-Partners, having a low degree of complexity and minimising contamination of the vacuum: the so-called through-wall stage.

DICK LARO, ELWIN BOOTS, JAN VAN EIJK AND LEO SANDERS

In the concept, a separation has been made between two vacuum levels: a clean/precision vacuum and a non-precision/dirty vacuum. The separation between the two is realised by a wall (see Figure 1). The design uses a Short Stroke-Long Stroke (SS-LS) stage configuration where the SS stage exerts its actuation forces through the wall. The precision vacuum contains the SS chuck carrying a wafer to be machined or inspected. In the non-precision vacuum a conventionally stacked LS x-y stage can be placed. The function of this XY stage is to enable a larger stroke for the short-stroke system. The vacuum underneath the separator plate is only required to minimise loads on the wall due to the pressure difference over a large area.

One of the challenges of the “through wall” concept lies in the development of new actuators. These actuators will have to act through the wall. This wall introduces a relatively large airgap. The typical airgap is assumed to be in the order of 5 mm. This 5 mm consists of space for the wall itself and its deflection and allows for a mechanical tolerance of 1 mm on each side.

System architecture

The performance of the through-wall concept has been evaluated by realising a demonstrator. The demonstrator's machine architecture was based on a separate force frame and sensor frame layout. The schematic layout of the dynamic architecture is shown in Figure 2. The reaction forces of the SS stage are transferred through the LS stage into the force frame. These SS reaction forces could excite internal dynamics within the LS stage, possibly limiting the bandwidth of the SS stage. By placing the sensors on a separate metrology frame with a low-frequency suspension, a mechanical filter is formed that reduces the “visibility” of flexible modes within the force frame and LS stage.

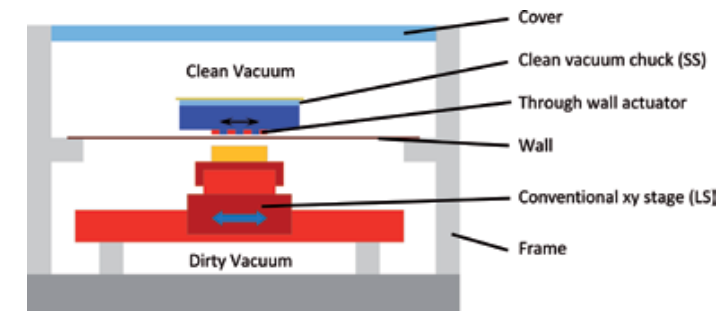
The SS chuck holds the wafer on which machining or inspection can occur. The SS stage is controlled in the six degrees of freedom (DoFs) of a rigid body. For an unconstrained rigid body, a minimum of six sensors and six actuators are needed to control the six DoFs. When more sensors or actuators are used than the number of controlled DoFs, the system is called over-sensed or over-actuated, respectively. A wafer chuck is typically square-shaped. The torsional mode of such a structure typically limits the achievable bandwidth in vertical directions (Z, Rx, Ry). Research [2] has shown that by using four actuators in vertical direction instead of the minimum number of three, the internal dynamics of the chuck are more favourably excited. This allows high bandwidths to be achieved for lighter, more flexible systems. To exploit this advantage, four vertical actuators are used. As a symmetrical mass distribution is beneficial for the applied over-actuation, four horizontal actuators are used as well.

AUTHORS' NOTE

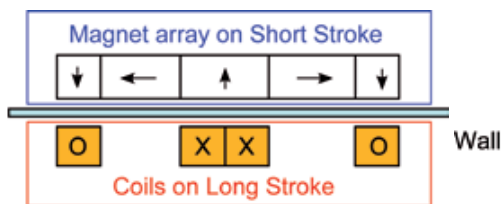
Dick Laro, system architect, Elwin Boots, mechanical developer, and Leo Sanders, director, all work at Eindhoven-based MI-Partners. MI-Partners is a company that performs contract R&D in the field of high-tech mechatronics. This article in part draws on the M.Sc. work by Elwin Boots when he was a Mechanical Engineering student at Delft University of Technology, the Netherlands. Jan van Eijk is professor emeritus of Advanced Mechatronics at Delft University of Technology and is owner of MICE bv, based in Eindhoven, the Netherlands. This article was, in part, based on a presentation at

the DSPE Conference, which was held on 4 and 5 September 2012 in Deurne, the Netherlands. The authors thank IBS Precision Engineering for supplying the eddy-current sensors and Magnetic Innovations for verifying the 2D simulations in 3D. This research has been conducted within the XTreme Motion project, part of the “Pieken in de Delta” programme of the Dutch Ministry of Economic Affairs.

d.laro@mi-partners.nl, www.mi-partners.nl,
www.micebv.nl, www.tudelft.nl



1



3

The SS is positioned with respect to the metrology frame using active control loops. To minimise transfer of disturbances to the SS stage, the connection in the form of stiffness to the outside world should be kept small. As the stage operates without cables, the dominant stiffness is present within the actuators. One of the goals for the actuator design is to keep the combined stiffness below 3 N/mm.

Actuator design

For the through-wall concept, the airgap will typically be larger than in a conventional system. Next to this, only one side is available for attaching coils. This requires the development of new actuators. To keep control of the stage simple, the goal is to develop 1-DoF actuators that do not require position-dependent control. The design of the actuators is based on “off-the-shelf” magnets to allow for a relatively short manufacturing time.

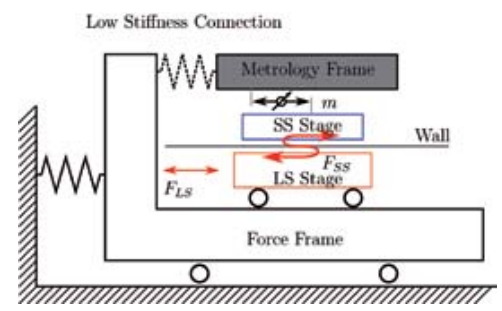
In-plane design

The in-plane actuator consists of a planar Halbach magnet arrangement and two coils (Figure 3). The Halbach arrangement is attached to the SS stage and “pushes” the magnetic field through the (non-ferromagnetic) wall towards the LS stage. Inside the LS stage the coils are situated. The SS and LS stages make relative displacements in the order of one millimeter. The magnetic design minimises position dependency of the propulsion force.

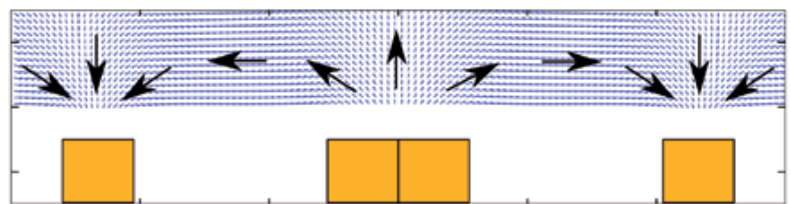
To optimise the actuator design, analytical equations for square magnets [3] were used. The magnetisation direction for the magnets has to be established within a fixed volume to achieve maximum propulsion force. To do so, the magnet area was divided into 1 mm² blocks, with each block having

its own magnetisation direction. For each block the magnetic field is calculated with horizontal and vertical magnetisation using the analytic formulas. The forces in the coil are then calculated by taking the cross product between the current density and the magnetic field. Finally, the total force and torque are calculated by numerical integration over the coil. These forces correspond to the horizontally and vertically magnetised block; other magnetisation directions can be calculated using combinations of the horizontally and vertically magnetised block. The magnet configuration that delivers the highest force is shown in Figure 4.

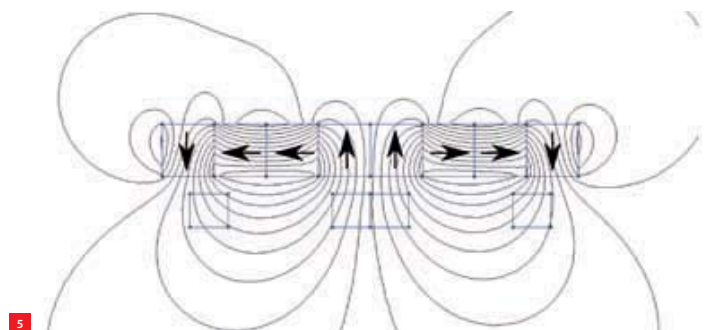
To be able to use off-the-shelf magnets, the configuration had to be simplified. The final configuration was chosen such that it can be fabricated out of just one type of cuboid magnets. The resulting magnetic field is shown in Figure 5. The design without active coil cooling is capable of generating a propulsion force of 60 N at a gap of 5 mm. When water cooling is applied to the actuator on the LS side and the magnet geometry is customised, the force can easily



2

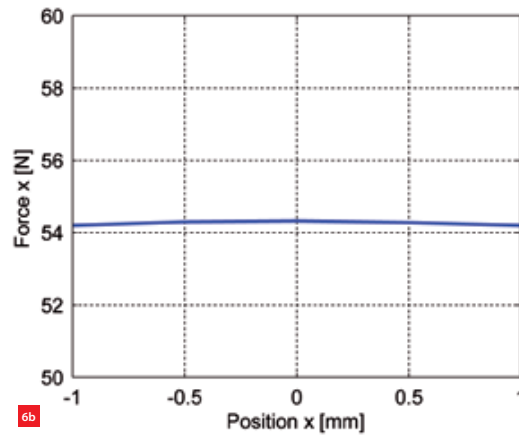
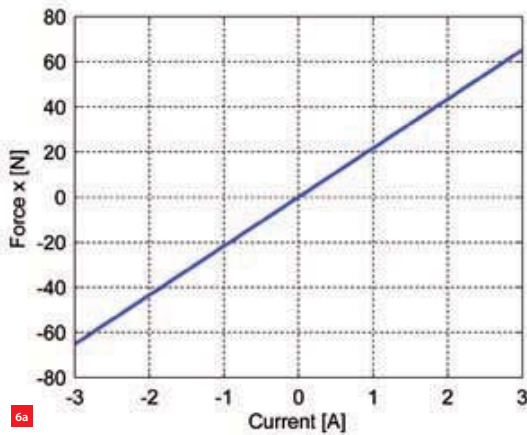


4



5

- 1 Through-wall vacuum stage concept, showing the separation between a precision/clean and a non-precision/dirty vacuum compartment, as well as the Long Stroke-Short Stroke stage configuration.
- 2 Dynamic architecture of the through-wall stage. The reaction forces of the SS pass through the LS stage into the force frame. The metrology frame is isolated with respect to the force frame.
- 3 In-plane motor concept, with a Halbach array on the SS stage and coils on the LS stage.
- 4 Optimal magnetic field for coils, to optimise propulsion force.
- 5 Magnetic field of designed in-plane actuator.



- 6 Measured forces of in-plane motor.
(a) Force versus current.
(b) Force versus position at $I = 2.5$ A.
- 7 Active magnetic gravity compensator for through-wall concept. Coils are present on LS side.
- 8 Working principle of active magnetic gravity compensator. Zero stiffness realised by ring-shaped magnet.

be increased by a factor of 4 within the same volume (100 mm x 150 mm x 40 mm). Specialised tools have been developed for actuator assembly, e.g. care should be taken to avoid demagnetisation during assembly.

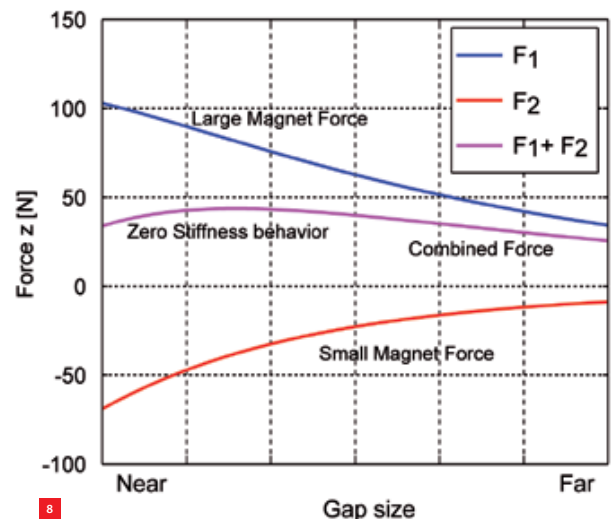
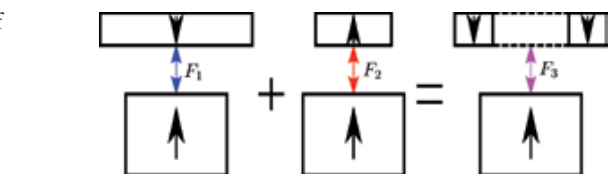
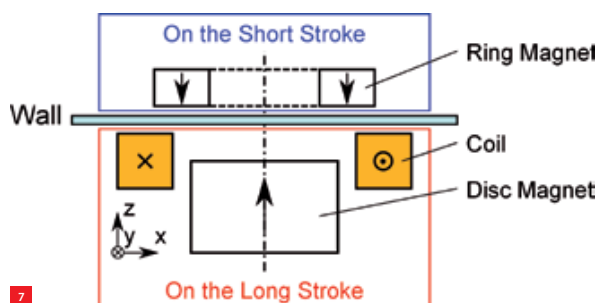
A measurement set-up has been realised to characterise the actuator. Figure 6 shows the measured force-versus-current characteristics. The position dependency is negligible and less than 1% of the actuation force.

Active magnetic gravity compensator

The active magnetic gravity compensator holds the weight of the stage using passive magnets and enables actuation using a coil on the LS side. The magnets minimise power consumption for carrying the weight, but risk the adding of actuator stiffness. As the long-stroke stage is envisioned to be a conventional stage without high requirements, the transfer of disturbances should be minimised. To realise this, a low-stiffness actuator between the SS stage and LS stage was required, featuring typically less than 1,000 N/m per actuator.

A zero-stiffness gravity compensator has been designed consisting of a disc and a ring magnet as shown in

Figure 7. The low-stiffness effect was realised by the hole in the center of the ring magnet. This hole can be seen as the superposition of a larger circular magnet combined with a smaller magnet polarised in opposite direction. The forces realising the low stiffness are graphically illustrated in Figure 8. The larger magnet with opposing magnetisation generates a repulsive force, F_1 , while the smaller magnet with attractive polarisation creates an attraction force, F_2 . The force F_2 has a steeper slope as the magnets come closer. By careful dimensioning, the sum of the force, F_3 , exhibits the desired zero-stiffness effect. A circular coil has been added to the design to enable actuation.



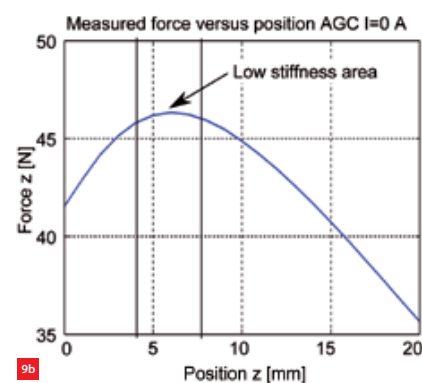
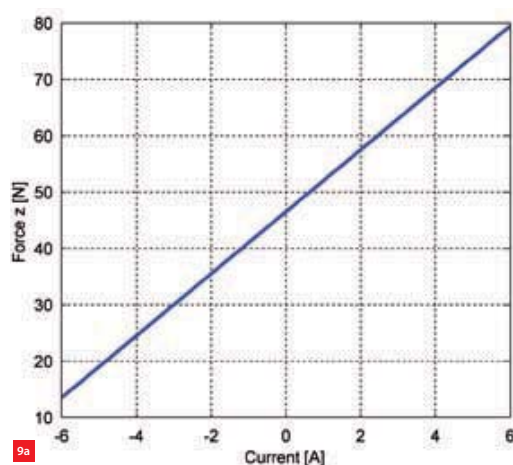
9 Measured forces of active magnetic gravity compensator.

(a) Force versus current.

(b) Force versus position at $I = 0$ A. This shows close-to-zero stiffness at 5 mm gap.

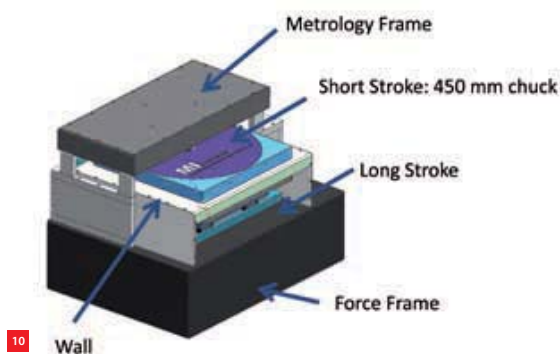
10 Overview of designed demonstrator.

11 Exploded view of the through-wall demonstrator. SS only holds permanent magnets. LS is driven by a screw spindle.



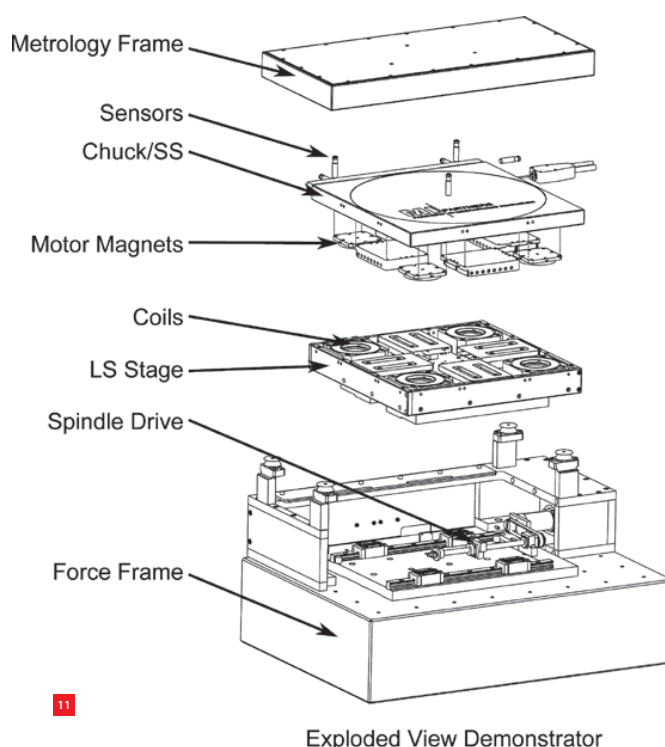
To optimise the design of the actuator, the influence of various parameters has been analysed. These parameters consisted of the ring's inner and outer diameter, its thickness, as well as the disc's diameter and thickness. The optimisation was performed using an axisymmetric FEM (finite-element model) analysis. In this model only the out-of-plane force and stiffness can be calculated. The in-plane stiffness can then be calculated using Earnshaw's theorem [4]. From this theorem it can be deduced that the out-of-plane stiffness is equal to twice the in-plane stiffness with the sign inverted. This shows that a low vertical stiffness will directly lead to a low in-plane stiffness as well. The location of the zero stiffness can be adjusted by changing the diameters, while the amount of force is dictated by the thickness of the magnets. For the final design of the actuator only off-the-shelf magnets have been used.

Figure 9 shows the measured force versus position and current. The figure clearly displays the zero-stiffness behaviour of the actuator. Each of the actuators will carry 46 N of gravity load.



Mechanical design

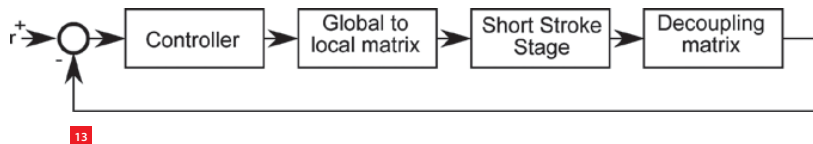
To demonstrate the potential of the through-wall concept, a demonstrator has been realised. The demonstrator consists of the following elements: the SS, the LS, the wall, a metrology frame and a force frame as depicted in Figure 10. The goal of the demonstrator is not to reach nanometer precision but to show the concept and use it as an exhibition demonstrator. The design consists of a 500 mm x 500 mm SS wafer chuck, making it compatible with the newest generation of 450 mm wafers. No wires run to the chuck and it contains the magnets for in-plane and out-of-plane





12 The demonstrator at an exhibition.

13 Control architecture of SS stage. Decoupling occurs around its center of gravity.



actuation. The demonstrator is not a vacuum system, but its components are vacuum compatible. An exploded view of the system is shown in Figure 11.

To measure the chuck, the metrology frame holds five eddy-current sensors and one laser interferometer. An additional eddy current is present for start-up purposes. The metrology frame is suspended on four rubber mounts. For the demonstrator system a suspension frequency between 10-15 Hz was selected. This is a trade-off between the filtering effect and practical stability of the frame as it will be used as an exhibition demonstrator.

On the granite base the LS stage is positioned. Due to the low stiffness of the actuators, vibrations on the LS stage only lead to small disturbance forces on the SS chuck. This allows the stage to be actuated by a simple screw spindle. Its position is measured by a linear encoder. Currently, the

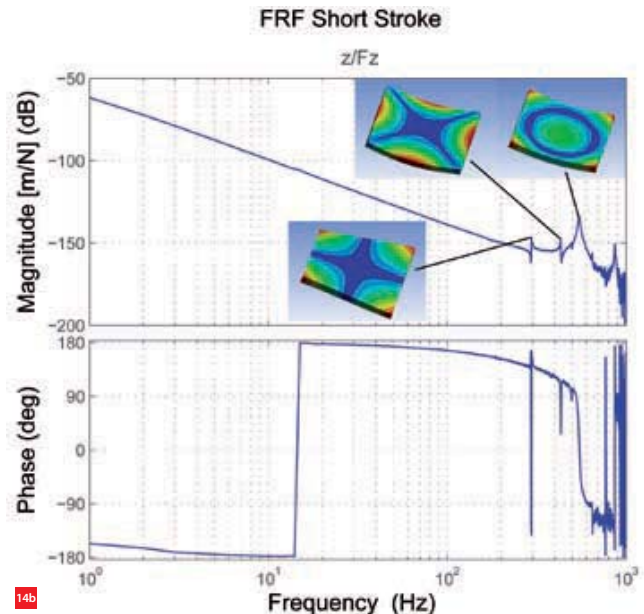
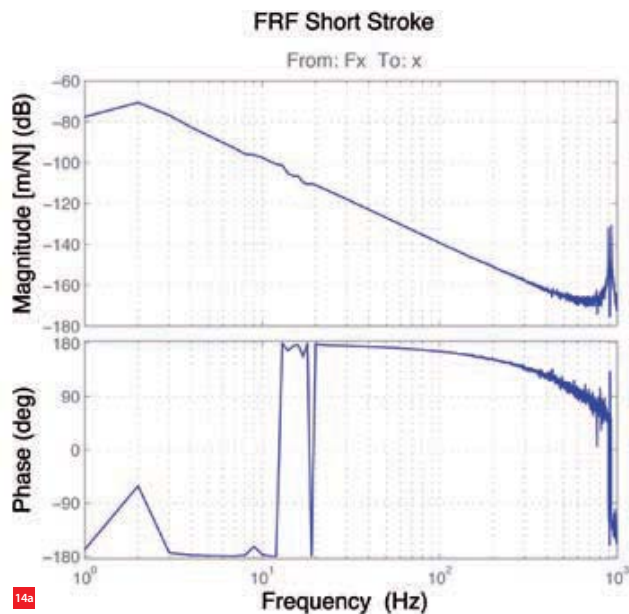
design has only one long-stroke direction, but a stacked XY stage can easily be added to the system to facilitate additional motion. Figure 12 shows a picture of the demonstrator at an exhibition.

Control results

To control the stage, the local measurements are decoupled around the centre of gravity of the chuck by use of a transformation matrix. The SS stage is controlled with six individually tuned PID controllers and forces distributed to the actuators by use of an actuator transformation. The layout of the control scheme for the SS stage is shown in Figure 13. The LS stage is controlled with respect to the force frame and obtains the same set-point as the SS stage, allowing it to roughly follow the motion of the SS stage.

The bandwidth of the SS stage was tuned to 100 Hz in all directions. The plant transfers in X- and Z-direction of the SS stage are shown in Figure 14. In Z-direction, the torsional modes of the chuck are only mildly excited and are hardly present in the FRF (Frequency Response Function). The main limitation is formed by the umbrella mode at 550 Hz. In X-direction, around 10 Hz excitation of the metrology frame can be seen; internal dynamics of the LS stage are not visible. The bandwidth-limiting modes are located at 900 Hz.

The position stability of the stage is in the order of a micrometer; this is mainly limited by the resolution of the eddy-current sensors as they have been selected to operate over a large range. By using a different sensing method, the performance of the stage can be improved to nanometer level. In Figure 15, the acceleration profile for a 10 cm set-point for a combined motion (LS+SS) is shown. The servo error of this set-point is also shown in Figure 15. The LS stage makes considerable errors that do not influence the tracking error of the SS stage. A frequency component of around 10 Hz can be seen in the servo error of the SS stage, which is caused by the excitation of the metrology frame by the set-point reaction forces.

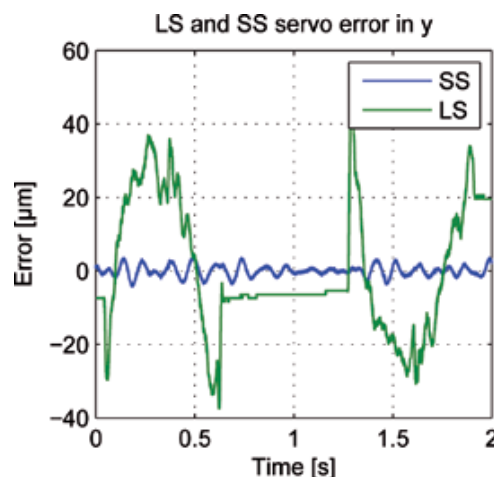
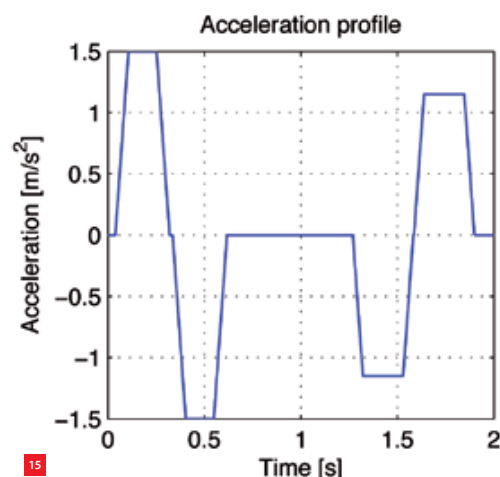


Conclusions & Outlook

The through-wall stage enables wireless actuation in a vacuum environment with promising performance. The application of over-actuation enables high dynamic performance for a relatively lightweight/flexible chuck. Integration of the system with a 6-DoF laser interferometer system will allow it to perform at nanometer level. Some form of wireless energy transfer will be required to allow for wafer clamping. At this moment, several customers have shown interest in the concept. MI-Partners is looking for cooperation with potential stage suppliers or OEMs for further development of the platform. ■

REFERENCES

- [1] J.W. Jansen. "Magnetically levitated planar actuator with moving magnets: Electromechanical analysis and design", Ph.D. thesis, Eindhoven University of Technology, 2007.
- [2] D. Laro, R. Boshuizen, and J. van Eijk. "Design and control of over-actuated lightweight 450 mm wafer chuck", *Proc. ASPE Control Topical Meeting*, 2010.
- [3] H. Allag, J.P. Yonnet, and M.E.H. Latreche. "3D Analytical Calculation of Forces between Linear Halbach-Type Permanent Magnet Arrays", *Electromotion*, 2009.
- [4] S. Earnshaw. "On the Nature of the Molecular Forces which Regulate the Constitution of the Luminiferous Ether". *Trans. Camb. Phil. Soc.* 7: 97-112, 1842.



14 Plant FRF of SS stage.

(a) In X-direction.

(b) In Z-direction.

15 Set-point tracking performance in horizontal direction for 10 cm set-point for given acceleration profile. Tracking errors on SS stage are unrelated to errors of LS stage.

EXCITING INTERNATIONAL MECHATRONICS EVENT

At the end of April, Eindhoven will be the stage of the High-Tech Systems conference and exhibition. Over the past year this international event around mechatronics and precision technology has gathered the support of the entire high-tech industry in the Netherlands, and collaborations with important partners in Flanders and Germany have started.

AUTHOR'S NOTE

Joost Backus works with Techwatch, one of the organisers of HTS 2013.

joost@techwatch.nl
www.techwatch.nl

JOOST BACKUS

The High-Tech Systems (HTS) conference is an initiative of the prominent independent technology organisations Brainport Industries, DSPE, Syntens (Enterprise Europe Network), FMTC (Flanders Mechatronics Technology Centre) and Techwatch. The ambition of the five organisers is to create a Western European high-tech conference/exhibition and to put this initiative on the global stage in the coming years. "We aim for an event that will grow in terms of visitor numbers and international importance every year," says René Raaijmakers, managing director of Techwatch. "We intend to invest in a strong platform that is of vital importance for the high-tech industry."

Lecture programme

Heart of HTS 2013 is a lecture programme focused on advanced mechatronics, precision technology and system engineering for the semicon, automotive, medical and agro&food sectors. Additionally, HTS 2013 will also address the theme of conceptual system engineering and model-

driven development. Other special lecture tracks will focus on the various computer-aided design techniques, such as physical modelling and finite-element methods. For decision-makers and technical management, the event features a special lecture track dedicated to international collaboration. ASML, Zeiss, Mapper, Philips Innovation Services, Süss MicroTec and others will be giving presentations about their experiences in international collaboration on high-tech system development. Apart from the general programme, HTS 2013 will be giving the floor to several side events from "third party" organisations and players in the high-tech market. For instance, Applied Piezo will organise their final symposium for the SmartPie research programme, focusing on system integration and control in piezo technology.

High-tech ecosystem

The organisers expect High-Tech Systems to strengthen the high-tech ecosystem in the Flanders-Germany-Netherlands area. This ambition is underlined by the tremendous support they received from many major technology (branch) organisations, such as BOM, Dutch Precision Technology, FEDA, High Tech NL (the merger of High-Tech Systems Platform and Point-One), NEVAT, Oost NV, RoboNED, the HTSM topteam, and Holland High Tech (all NL), as well as VDE, NRW Produktion, Spectaris, In|Die Regionruhr (all DE), and FMTC (BE).

Germany

The organisers decided to approach international target audiences step by step and first of all focus on Germany for the 2013 edition. Fortunately, this initiative received support from neighbouring regions almost immediately. In the past

Ambitious programme

High-Tech Systems 2013 on 24 and 25 April in Eindhoven, the Netherlands, features a peer-reviewed high-quality lecture programme, a two-day business fair with ample time to network, an international matchmaking programme, as well as a spectacular pre-event tour programme for hands-on visits to the Dutch/Belgian tech ecosystem. There is a dedicated job fair specially for students and starters in the technology sector.

WWW.HIGHTECHSYSTEMS.EU

months, as mentioned, several German technology networks have decided to actively support HTS 2013, and there is strong support from the Dutch consulates, embassies and NBSOs (Netherlands Business Support Offices), which are actively promoting the conference. The Enterprise Europe Network will enable international matchmaking during the event.

Tour

To make a visit to the conference city of Eindhoven more attractive for international guests, HTS 2013 will have a special "pre-event" tour programme, featuring visits to exciting high-tech companies ASML, FMTC, Frencken, Holst Centre, Imec, Mutracx, NTS, NXP, Omnicadar, Philips Innovation Services, Shapeways, Sorama, VDL ETG and Xpress Precision Engineering, as well as to the High Tech Campus Eindhoven. The tour will offer splendid networking possibilities.

Marketing power

The first ideas for HTS date back to 2011. Brainport Industries, DSPE and Syntens asked FMTC and Techwatch to take their existing conference Hightech Mechatronica to an international level. Hightech Mechatronica has been organised since 2007 and was known for its high-quality conference programme and high-level audience of engineers, technical management and decision makers in the high-end system development market.

"The cooperation with DSPE enables Techwatch to combine the marketing power of DSPE's Mikroniek magazine with our titles Bits&Chips and Mechatronica&Machinebouw", says Techwatch's René Raaijmakers. The support of this marketing power, the help of an abundance of network organisations, top high-tech exhibitors, a splendid conference programme and an interesting tour, give the organisers the confidence to expect an audience of 3,000 visitors. ■



Air-Bearing Motion Solutions for Test and Inspection



Aerotech air bearings are the highest-performance positioning systems available, and we have been at the forefront of positioning technology since 1970. Let us show you how our systems stack-up against the competition.

Aerotech Air-Bearing Benefits:

- Highest possible scanning and positioning performance for demanding test and inspection
- Noncontact motors and optical encoders mean no wear or reduction in performance over time
- Outstanding stiffness for heavy or offset loading
- Ideal for cleanroom use



ABL1500XYZ
3-axis
air-bearing
stage



ABRS
rotary
air-bearing
stage



AirLift115
air-bearing
lift stage



*Dedicated to the
Science of Motion*

Ph: +44 (0)118 940 9400
Email: sales@aerotech.co.uk
www.aerotech.com

Aerotech Worldwide

United States • France • Germany • United Kingdom
China • Japan • Taiwan

AH1212A_TM

INNOVATIVE TECHNICAL CERAMIC SOLUTIONS

In mid-December 2012, Formatec Ceramics, based in Goirle, the Netherlands, organised the Ceramic Injection Moulding seminar. The programme included presentations, such as the unique 3D printing of products using technical ceramics, and guided tours showcasing the fine art of injection moulding using ceramic material.

1 Close to 100 guests attended the technology seminar organised by Formatec Ceramics.



The programme of the well-attended seminar (see Figure 1) was opened by Michiel de Bruijcker, Managing Director of Formatec Ceramics, followed by a presentation by Joep Brouwers, Vice Director of Brainport

Development, highlighting successes in the open supply chain in the province of Noord-Brabant, the heart of the Dutch high-tech manufacturing industry.

Silicon nitride

A short film featuring a jet engine-powered scale model plane illustrated the use of silicon nitride (Si_3N_4) in a microturbine, which requires extremely high levels of hardness, durability and thermal shock resistance; the specifications were a turning speed of 120,000 rpm and a maximum temperature of 850 °C. Having already gained experience with this material, last year Formatec decided to develop its own feedstock, which is required in order to be able to process Si_3N_4 by injection moulding. Ceramic Injection Moulding makes it possible to create more complex shapes, which is a step forward compared to the

current pressing technology. Silicon nitride is used in, for example, medical products and specific machine parts that require a high level of durability. Polishing the material at the final stage ensures an exceptionally smooth surface. For example, Formatec now also manufactures luxury silicon nitride watchcases for clients in Switzerland.

Micro injection moulding

The small dimensions of the ceramic products that Formatec is able to manufacture using injection moulding are impressive. To illustrate this, a fibre optic connector was shown with 64 holes in a 2 x 2 mm² area (see Figure 2). Each hole is as small as 125 µm and comes out of an injection mould, no less! The trick here is to optimise the material's granular structure, which Formatec has managed to do. Thanks to this micro injection moulding technique, eight million material granules can be perfectly positioned – within an extremely short time frame – in each cubic millimeter.

DLP printing

Formatec founder Peter Kuijpers presented the latest development: 3D ceramic printing. 3D printing is already being used in various forms and numerous materials, including plastics and metals. Formatec conducted extensive

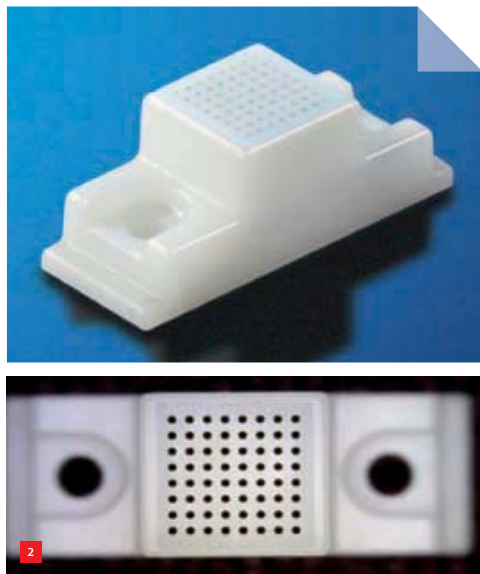
EDITOR'S NOTE

This report was contributed by Formatec, based in Goirle, the Netherlands.

www.formatec.nl

Table 1 Specifications of the Formatec DLP printer.

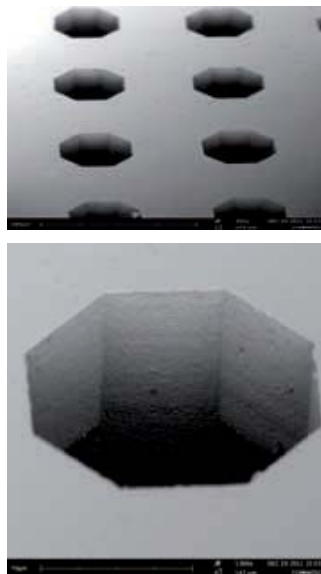
Resolution	40 µm
Layer thickness	25 - 100 µm
Speed	2.5 mm/h
DLP Chip	1980 x 1080 pixels
Building platform	76 x 43 mm ²



2 Manufactured by means of zirconia micro injection moulding: a fibre optic connector with 64 holes within a $2 \times 2 \text{ mm}^2$ area. The close-ups show the degree of finish of the holes.

3 Schematic of Formatec's 3D printer.

4 A 3D printed product manufactured with Formatec's DLP printer.



research into Digital Light Processing, developing a printer that illuminates and sets the ceramic material that is blended with a photopolymer, layer by layer; Figure 3 shows a schematic of this linear system. The main advantage of this is the option of high-resolution printing. Combined with the infinite number of shapes that are possible with 3D printing, this offers unique possibilities.

When the so-called green product comes out of the printer, it undergoes the debinding and sintering process that Formatec has successfully applied for years. This produces ceramic products with the well-known high-quality properties that no other technique can produce. It is ideal for prototypes or small series, as no mould is involved. Moreover, it cuts lead times considerably.

The Formatec DLP printer is targeted at producing small high-precision parts. Table 1 lists some specifications. As with any technology, there are advantages as well as disadvantages; see Table 2.

Table 2 Advantages and disadvantages of 3D ceramic printing "the Formatec way".

Advantages	Disadvantages
No tooling costs	Limited wall thickness, max. 2.5 mm
Series production for complex-shaped products	Relative slow production process
Prototype with full functional properties	Limited selection of ceramic types (to date, only Al_2O_3 and ZrO_2)
Extremely high design freedom	
Low costs for design changes	
High precision through high resolution	
Rapid throughput	

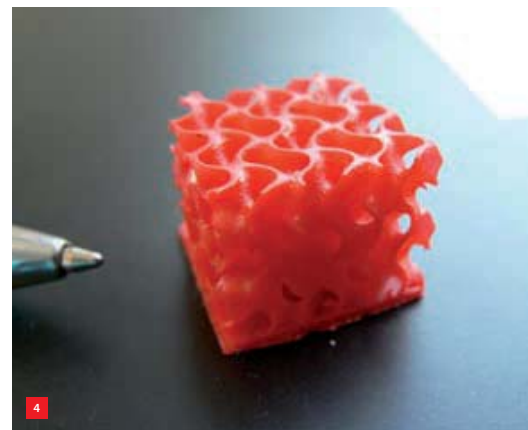
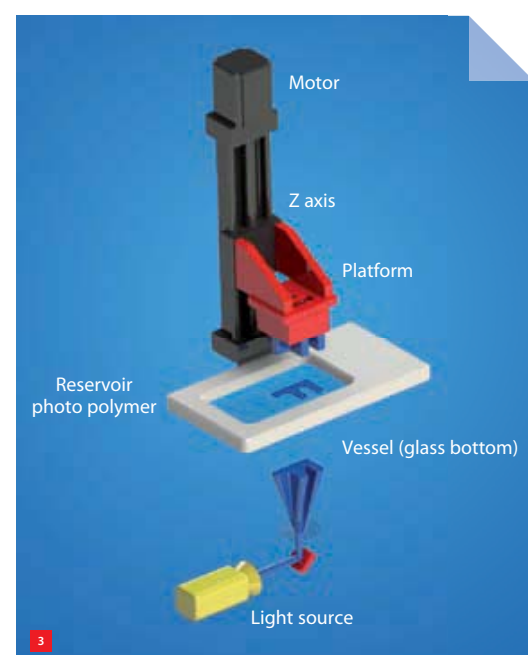


Figure 4 shows an example of a 3D printed ceramic product.

Outlook

By designing, engineering and constructing the DLP printer for ceramics, Formatec made a first step. For the months to come, Formatec has committed itself to an ambitious development plan. Working on material availability, material characterisation and delivering the first commercial products, are among the goals for 2013. ■



NOVEL TURRET OPTICS DESIGN

Belgium-based laser micromachining specialist Optec has developed an automatic multi-wavelength laser delivery solution based around Aerotech micropositioning systems and motion controls. The high-repetition multi-wavelength femto/picosecond micromachining project was designed and built for the prestigious Karlsruhe Institute of Technology (KIT).

Optec, based in Frameries, Belgium, is a leading global supplier of state-of-the-art laser micromachining systems used throughout industry and research. For a recent multi-wavelength and high-repetition femto/picosecond workstation (see Figure 1), commissioned by the prestigious Karlsruhe Institute of Technology (KIT) for its Karlsruhe Nano Micro Facility (KNMF), they developed a novel Turret Optics (TO) design to deploy and index the system's three galvo heads with near-perfect sub-micron repeatability – using a combination of Aerotech ALAR series rotary and PRO series linear vertical stages. When compared to alternative In-Line Optics (ILO) designs for such machines that need to switch rapidly and automatically between wavelengths for the varied use they must perform, the TO system not only provides superior positioning performance but is also much more compact; and with fewer positioning axes, requires less complex control, has faster development and build timescales and lower component costs.

In-Line Optics design

A typical ILO design (see Figure 2) would employ the three galvo heads, fixed optics and diagnostic equipment on separate Z-axis positioners, in line and above the X-axis translation stage of the machine which is used for part positioning. For a machine that can access the complete area of a part under test that measures 300 mm x 300 mm, the X-axis would need to have a travel range of around 1,000 mm. The overall machine size is perhaps only a problem for research sites or production floors with limited space, but the real problem is the limited overall precision attainable through the machine geometry. The spacing between the

optical heads and the parallelism between each Z-axis, as well as each stage's straightness and flatness deviations, all contribute to compound registration errors which reduce the overall ability to perform work accurately. The complexity of coordinating the various axis controls for multi-wavelength work can also be cumbersome and time consuming.

Turret Optics design

For the Optec TO design, the optics are mounted as a balanced load with the three galvo heads and diagnostics equipment suspended below a rigid post which is attached directly to the high-precision ALAR rotary axis that features direct-drive technology and benefits from zero backlash, high stiffness and high axial load capacity. The rotary stage is mounted, via a right-angle bracket, to a single heavy-duty Z-axis stage with an integral counterbalance and brake for safety and complete stability. With the rotary stage's large aperture, the laser and other services can be centrally delivered to the galvo heads. This arrangement ensures that the arrival point for all laser beams is from the same point above the work and that registration is dependant only essentially upon the angular repeatability of the rotation stage.

This elegant solution, similar in concept to a microscope objective turret and controlled by the inherent precision of the rotary stage (which returns a repeatability of ± 0.5 arcsec or ± 0.3 microns over its 300 mm pitch circle diameter), translates into an overall machine repeatability around a quarter of the ILO solution. Furthermore, the X-axis stage used for part positioning needs only to have a travel range of marginally more than 300 mm for the same

EDITOR'S NOTE

This article was contributed by Aerotech, a supplier of high-precision, high-throughput motion systems used in manufacturing production, quality control and R&D.

www.aerotech.com



working area as the ILO example, saving considerable space. Furthermore, the control and set-up time is substantially reduced.

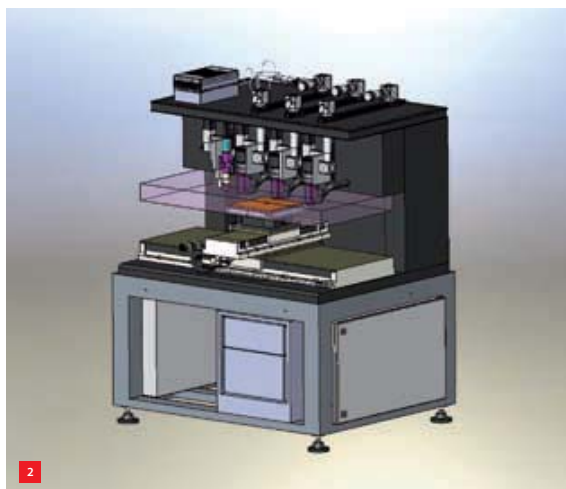
Exceeding the specification

Rod Andrew of Optec, who defines his role as a 'system architect', wanted to be absolutely sure that the Aerotech stages and controls would deliver the very stringent specifications required for his design concept. "At the tendering stage of the project, a series of tests were performed on an ALAR-100 rotary stage which was kindly loaned for evaluation. The combination of physical tests, including a moment load test, and calculations backed up by Aerotech's considerable technical support efforts, convinced us that we could meet and exceed the specification; and with our simplified design, submit a very competitive tender." Andrew comments further, "The machine has now been delivered and the TO concept works very nicely with sub-micron repeatability – we recorded these levels at the test phase on the final machine with the on-board inspection microscope at 1,000x magnification."

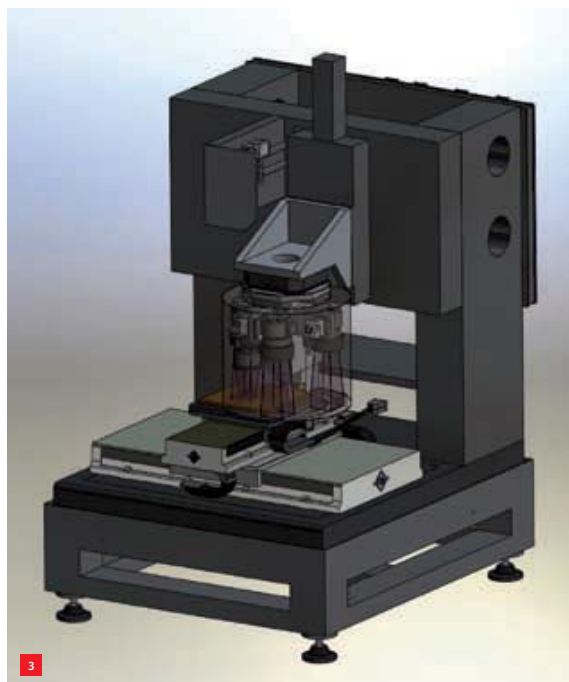
No thermal impact

The specification for the ultrafast and high-repetition femto/picosecond laser machining system, which was funded by the KNMF, is extremely wide-ranging. KNMF is focused on providing open and, for public work, free access to multi-material state-of-the-art micro- and nanotechnologies for users from industry and academia, worldwide. The Optec workstation is now installed and is working to the complete

- 1 Optec's multi-wavelength ultrafast laser micromachining workstation for KNMF.
(a) Side view.
(b) Front view.
- 2 Rendering of the In-Line Optics (ILO) design for the multi-wavelength workstation.



■ MULTI-WAVELENGTH ULTRAFAST LASER MICROMACHINING WORKSTATION



3 *Rendering of the Turret Optics design for the multi-wavelength workstation.*

satisfaction of Dr Wilhelm Pfleging, who is head of the Laser Technology Division at KIT. He comments, “By using this specially configured workstation (e.g. fundamental and 2nd and 3rd harmonics, tunable pulse length, etc.), complex and high-speed laser micro- and nanostructuring of multi-material systems such as biomaterials, transparent materials as well as materials for energy-storage devices, is possible without inducing thermal impact. High

repeatability and reproducibility is also achieved.” The broad range of applications open to KNMF for the new multi-wavelength femto/picosecond laser system is also impacted on several European research initiatives, including the Smart production of Microsystems based on laminated polymer films (SMARTLAM) and ECO-efficient LASER technology for FACTories of the future (ECO-LASERFACT). ■

INFORMATION

WWW.OPTEC.BE
WWW.KNMF.KIT.EDU







Ceramic on the right spot

Poppenbouwing 35
4191 NZ Geldermalsen
T: +31(0)345 - 58 01 01
F: +31(0)345 - 57 72 15



WWW.CERATEC.NL
E: ceratec@ceratec.nl
I: www.webshop.ceratec.nl

PRECISION JOINING OF PLASTICS AND METALS

AUTHOR'S NOTE

Frans Zuurveen is a freelance text writer who lives in Vlissingen, the Netherlands.

Miniaturising products often means that different materials have to be joined with high precision and guaranteed reliability. To create a reliable joint, you need to have a thorough knowledge of the material properties and access to proper joining technologies. At Mikrocentrum's Micro-joining seminar late last year, German, Belgian and Dutch specialists shared their experiences concerning various precision-joining technologies.

FRANS ZUURVEEN

Micro-joining can be defined as the joining of two sheets of material, of which one is thinner than 0.5 mm, or the joining of differently formed objects with a resulting joint diameter of less than 1 mm.

Technologies facilitating such micro-joints include welding, adhesive bonding, ultrasonic bonding, soldering and brazing. Besides conventional heating methods, lasers or electron beams can be applied to create a melting zone. Ultimately, with all these technologies, it is the reliability of the joint that plays the most important role.

Lifespan expectations

The Micro-joining seminar was held on 6 December 2012 in Eindhoven, the Netherlands. Jan Eite Bullema of TNO explained the importance of reliable joints in electronic and electrical products. Lifespan cannot always be predicted, as illustrated by the Voyager 2 satellite which was launched in 1977. It was initially meant to have an operational lifespan of five years, but even after 35 years the electronics still work satisfactorily.

In his lecture, Bullema outlined the reliability and lifespan expectations of LED products and solar cells. For the latter, he compared soldering with conductive adhesive bonding. The adhesive used for this contains extremely fine silver grains. Failure mechanisms in solder joints include fatigue due to temperature cycling, creep under permanent load, corrosion due to galvanic processes and brittle fatigue caused by drop or shock.

Characteristic	Sn/Pb Solder	ECA / ICA
Volume Resistivity	15 $\mu\Omega$ / cm	350 $\mu\Omega$ / cm
Typical Junction R	10 - 15 mW	< 25 mW
Thermal Conductivity	30 W / m.K	3,5W / m.K
Shear Strength	15 MPa	14 MPa
Finest Pitch	300 μ m	150 μ m
Processing Temp.	215 $^{\circ}$ C	< 150 $^{\circ}$ C
Environmental Impact	Negative	Very Minor
Thermal Fatigue	Yes	Minimal

1

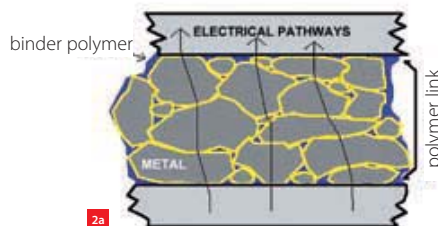
1 Comparison of the properties of soldered and adhesive-glued joints (ICA: isotropically conductive adhesives, ECA: electrically conductive adhesives).

2 Conductive adhesives in solar panel interconnections.

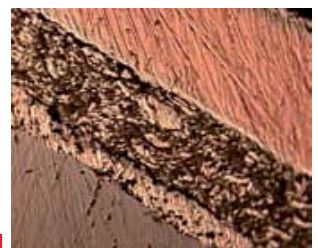
(a) Diagram of the conductive mechanism in conductive epoxy adhesive with silver grains.

(b) A silver-plated copper tab glued to silver-plated silicon (lower left) in a solar cell.

When standard soldering techniques are used to interconnect thin crystalline silicon solar cells, they may warp and are very likely to break. Applying a conductive adhesive prevents these unwanted effects from happening. Figure 1 compares the properties of soldered and adhesive-glued conductive joints. Improved reliability and a lower processing temperature come at the expense of lower electrical and thermal conductivities. Damp, heat and temperature cycling tests, however, show no degradation of the conductive adhesive joints. Figure 2a shows the conductive mechanism in epoxy adhesive with silver grains



2a



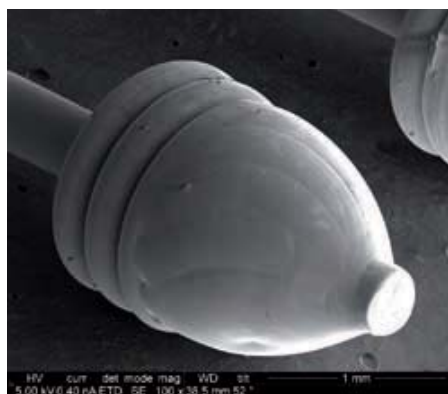
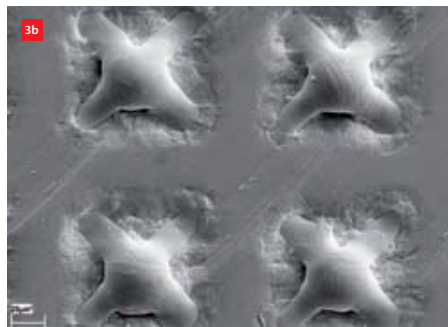
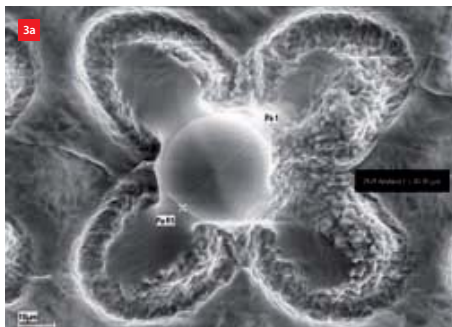
2b

3 Using an electron beam for micro-treating a titanium alloy surface to improve the bone ingrowth mechanism.

(a) An X-like pattern is created; the ball shape in the centre is due to the surface tension of molten metal.

(b) Patterns in a rectangular grid improve the ingrowth behaviour of bone tissue in implants.

4 Electrodes in Philips high-intensity discharge lamps connected and formed by a laser.



5 A medical 23 gauge injection needle with an outside diameter of $641 \pm 6 \mu\text{m}$ and inside diameter of $337 \pm 19 \mu\text{m}$. The Inox needle is epoxy adhesive-bonded in a polypropylene Luer lock coupling hub. (Courtesy of LCS Adhesive Bonding)

and Figure 2b shows a silver-plated copper tab glued to silver-plated silicon in a solar cell.

Despite the promising properties of gluing with a conductive adhesive, extra attention has to be paid to the curing efficiency, because this really determines the long-term behaviour. Improper curing may lead to accelerated failure due to outer constraints.

Electron beam structuring of titanium

The bone ingrowth behaviour of medical implants made from titanium alloys can also be considered a micro-joining issue. Christian Otten from RWTH Aachen University described how an electron beam can micro-treat a titanium alloy surface to improve the bone ingrowth mechanism.

For his experiments, Otten used a Focus MEBW 60 electron beam welder with an acceleration voltage of 60 kV and a 2 mA spot diameter below 30 µm. The beam describes an X-like pattern consisting of four lines, each with a length of 50 µm. The surface tension of the molten metal creates a ball shape in the centre of the X (see Figure 3a) with a diameter of about 30 µm. By creating periodic structures on a surface of TiAl6V4 titanium alloy in a rectangular grid (see Figure 3b), bone tissue is better able to grow into this artificial surface. The ingrowth behaviour of bone tissue in this titanium alloy can be tested using fluorescent

pigmentation which makes the actin and integrin adhesion proteins visible. The formation of these proteins is typical of ingrowth behaviour.

Laser welding in light products

In his lecture, Jurgen Adriaensen disclosed that Philips Turnhout in Belgium has about 170 lasers in use for a number of different purposes, including welding components for lighting products. In many cases, such welds have to meet micron accuracy range requirements. The Philips GTDM laser laboratory is equipped to optimise laser welding processes and has a range of (re)sources at its disposal: pulsed NdYag lasers, CO₂ lasers up to 1.5 kW, diode lasers up to 2 kW and Q-switched lasers for 1,064 nm wavelength. Figure 4 shows some examples of light products precision-machined by lasers at the Philips Lighting factory in Turnhout.

Adhesive bonding

Jan Lambrechts gave a lecture on the many advantages and disadvantages of adhesive bonding. He is an independent consultant in adhesive bonding technology who established the Belgium-based LCS Adhesive Bonding, which provides support at every stage of an adhesive bonding, encapsulation, sealing and coating project.

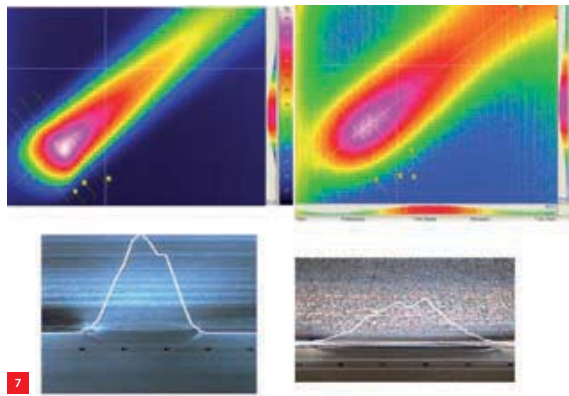
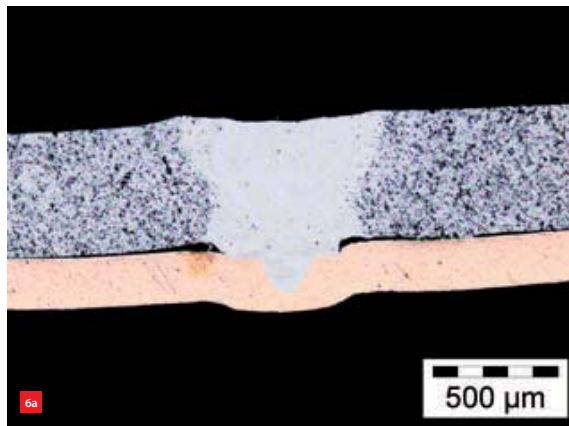


6 Micro-welding metal sheets.

(a) Connecting a 0.5 mm thick Al sheet to a 0.3 mm thick Cu sheet with a linear weld seam.

(b) The zone between these two curves guarantees a stable linear welding process. (Courtesy of Fraunhofer ILT)

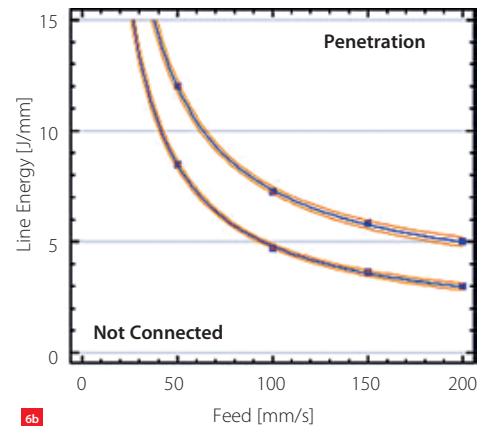
7 A comparison between welding PC (left) and welding PBT. Speed 100 mm/s, beam power 16.4 W (PC), 47.8 W (PBT). Colours indicate relative temperature measured by the Thermosensorik IR camera. The transversal temperature distributions are shown below. (Courtesy of Fraunhofer ILT)



He described an interesting example of adhesive bonding: the gluing of a medical injection needle with a smallest diameter of 180 µm (gauge 34) in a polypropylene Luer-lock coupling hub (see Figure 5). With this universal coupling system, the needle can be connected to a medical syringe in a fluid-tight manner. A UV-hardening high-speed adhesive bonding system is used with a hardening time of less than one second. A glue such as this has to comply with the stringent demands of ISO 10993 and the FDA (Food and Drug Administration). Furthermore, the glued products have to be able to withstand modern high-tech sterilisation methods. What's remarkable is that many millions of these adhesive-bonded disposable products are manufactured in one factory every day with 100% quality control.

Research in laser micro-joining

Benjamin Mehlmann is a research engineer at the Fraunhofer Institute for Laser Technology in Aachen, Germany. Here, laser beam sources and beam manipulation strategies are being investigated to optimise welding processes. An important aspect of these activities is the application of process simulation with computer models for heat distribution.



In his lecture, Mehlmann first pointed out the differences between welding thermoplastics and metals. When welding two sheets of CRP (Carbon Reinforced Plastic), the joining area has to be visible to the laser beam, which means that the upper joining partner needs to have a transmission ratio of at least 25%. By contrast, the lower partner must provide a high absorption for the laser radiation, which is mostly achieved by carbon black filling. A third factor to consider is the application of sufficient clamping force.

Translucency when micro-welding metal sheets is impossible, of course. Here, the weld is the result of creating a melting zone that extends into the lower sheet through the upper sheet, as illustrated by the welding of aluminium on copper (see Figure 6a). Such a welding process is only stable in a small working range because an excessive beam feed and line energy causes penetration of the sheets, whereas an insufficient value for these parameters prevents the two sheets from connecting properly (see Figure 6b).

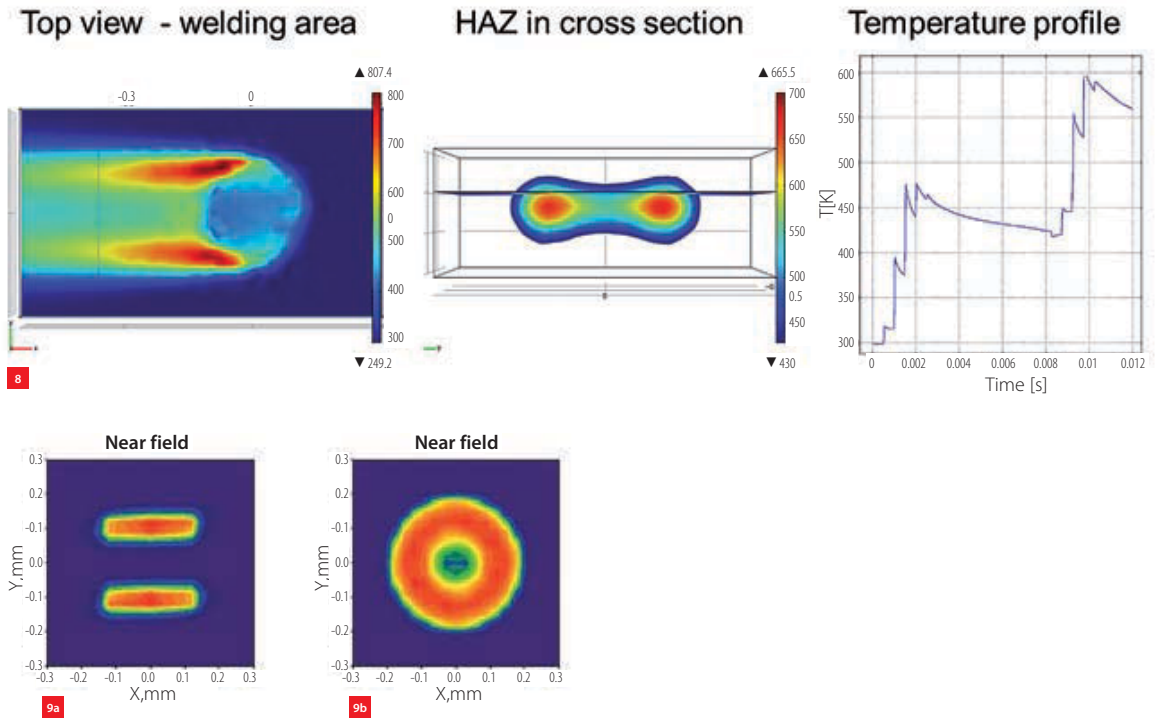
Beam intensity in detail

Andreas Roessner of Fraunhofer ILT used a Thermosensorik infrared camera to study the relative temperature distribution across a plastic surface during welding. Figure 7 shows these – relative – temperature distributions when comparing the optimised welding of PC (polycarbonate) at a speed of 100 mm/s using a beam of 16.4 W with the welding of PBT (polybutylene terephthalate) using a beam of 47.8 W. Local transversal temperature distribution curves show a widened welding zone for PBT due to scattering.

8 Computer calculation results based on the heat conduction Equation 1. Parameters: spot = 80 μm , power = 4 W, speed = 50 mm/s, frequency = 1,000 Hz. HAZ: heat-affected zone.

9 Beam shaping strategies. (Courtesy of Fraunhofer ILT) (a) With two separate lasers. (b) With a doughnut-shaped laser beam.

10 Spatial power modulation by optical beam deflection in two orthogonal directions, resulting in Lissajous figures on the workpiece. (Courtesy of Fraunhofer ILT) (a) Frequency ratio is 2:3, phase difference is 0. (b) Frequency ratio is 3:4, phase difference is $2/3 \pi$.



To predict the optimisation of the welding of polymers, a process simulation computer program was developed based on the following heat conduction equation:

$$\frac{\partial(\rho c_p T)}{\partial t} + \nabla \cdot (K \nabla T) = Q \quad (1)$$

where ρ = mass density, c_p = specific heat capacity, K = heat conductivity and Q = heat source value. Figure 8 shows some results.

Beam manipulation

The Fraunhofer Institute has also investigated various beam manipulation strategies with variations in time and space. Figure 9 shows two forms of optical beam shaping by using different lenses or other optical elements. Figure 9a shows the intensity distribution of a combination of two laser systems, each with a line optical system. Figure 9b shows a laser beam shaped like a doughnut.

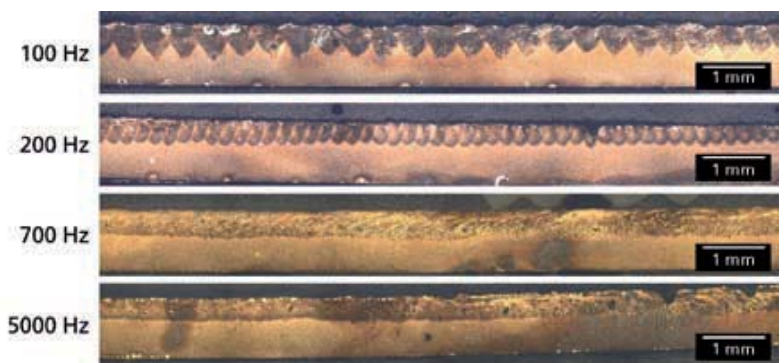
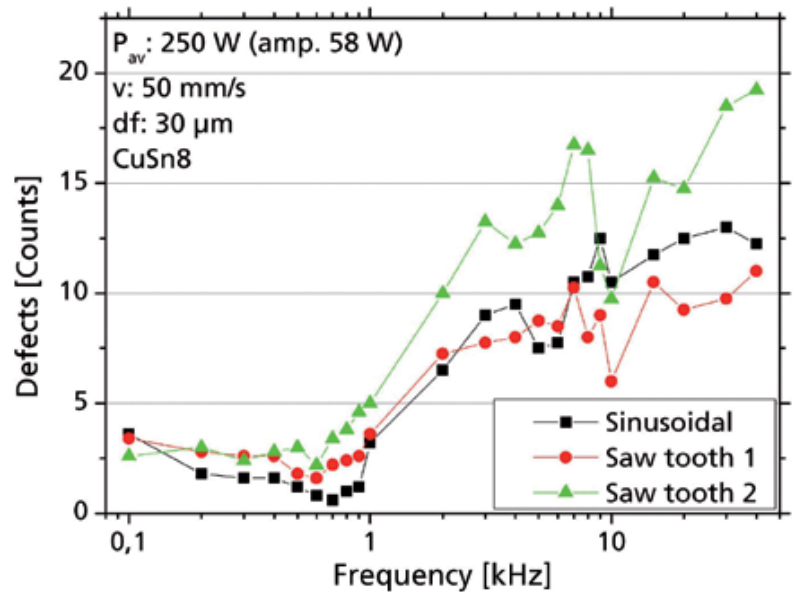
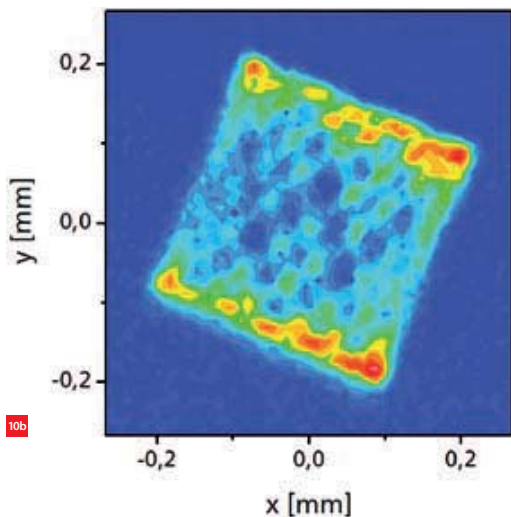
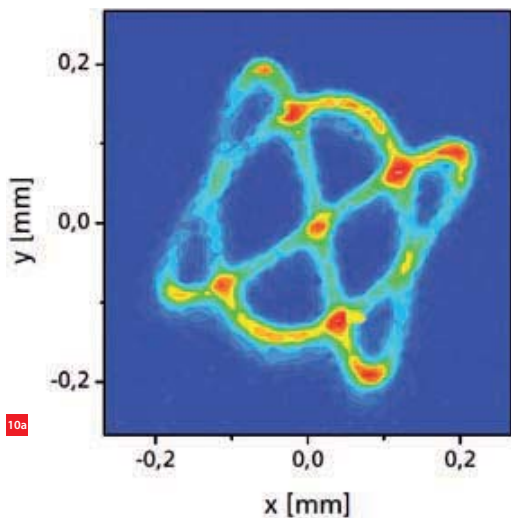
Figure 10 shows examples of spatial power modulation. In this case, normal-shaped beams with a focus diameter of less than 0.2 mm were used. These were optically deflected with high frequencies in two orthogonal directions, with Lissajous figures as the obvious results. In Figure 10a, the difference in phases is 0 and the frequency ratio is 2:3. In Figure 10b, the frequency ratio is 3:4 with a phase difference of $2/3 \pi$. This kind of spatial power modulation introduces

more parameters into the welding processes, adding an extra mechanism to adjust the power input into the workpiece. For polymers, this allowed to adapt the process to the physical and chemical properties of the materials. For metal welding, larger melt pools could be achieved without increasing power and welding speed.

Micro-joining copper

One of the research areas of the IFSW institute in Stuttgart, Germany, was the welding of copper with two different lasers: IR with a wavelength of 1,030 nm and green with a wavelength of 515 nm. Modulated and continuous laser beams were combined. Ultimately, the combination of a 500 Hz modulated IR spot with a continuous green spot gave the best results: a smoother weld seam with the lowest number of ejections due to holes.

The Aachen Fraunhofer Institute investigated the welding of CuSn8 with a temporal sinusoidal or saw-tooth power-modulated IR laser (see Figure 11). The best quality was achieved at a frequency between 600 and 800 Hz with a sinusoidal wave. Figure 12 shows pictures of longitudinal cross sections at various modulation frequencies. The pictures for 100 and 200 Hz look like spot welding, due to the low frequency of the modulation. The laser power in those cases falls under the threshold for deep welding. The picture for 700 Hz shows a nearly steady welding depth without defects such as ejections or pores.



To conclude

The introduction mentioned welding, adhesive bonding, ultrasonic bonding, soldering and brazing as technologies that have to be considered when talking about micro-joining. Only some of these technologies were dealt with in the seminar, but the participants learned that soldering can now be considered an old-fashioned technology because of its unreliability. At the other end of the micro-joining technology spectrum, laser joining wins where applicability is concerned because of its highly accurate way of dosing heat in relation to position, space and time.

In the middle of this spectrum comes adhesive bonding, with the outdated impression of a rather amateurish technology because of its reputation of unreliability: “collapses as time elapses”. However, seeing as airplanes fly year after year with bonded aluminium sheets, the fixed idea of unreliable adhesive joints has to change drastically. The symposium learned that to achieve a reliable adhesive joint, bonding parameters need to be monitored carefully. The fact that many millions of glued medical injection needles are produced every day is clear proof of this. ■

11 Measurement results from welding CuSn8 with a sinusoidal or saw-tooth power-modulated IR laser. The best results are achieved at a frequency between 600 and 800 Hz. There are more defects at higher frequencies. (Courtesy of Fraunhofer ILT)

12 Pictures of longitudinal copper sheet cross sections at various modulation frequencies. According to Figure 11, a frequency of 700 Hz shows a nearly steady welding depth without any defects. (Courtesy of Fraunhofer ILT)

CPE COURSE CALENDAR

COURSE	CPE points	Provider	Starting date (location, if not Eindhoven)
--------	------------	----------	---

BASIC

Mechatronic System Design (parts 1 + 2)	10	HTI	10 June 2013 (part 1) 4 March 2013 (part 2)
Construction Principles	3	MC	15 May 2013 29 October 2013 (Utrecht)
System Architecting	5	HTI	11 March 2013
Design Principles Basic	5	HTI	29 May 2013
Motion Control Tuning	6	HTI	17 April 2013

DEEPENING

Metrology and Calibration of Mechatronic Systems	2	HTI	18 November 2013
Actuation and Power Electronics	3	HTI	23 September 2013
Thermal Effects in Mechatronic Systems	2	HTI	11 March 2013
Summer school Optomechatronics	5	DSPE + HTI	24 June 2013
Dynamics and Modelling	3	HTI	25 November 2013

Specific

Applied Optics	6.5	MC	7 March 2013
	6.5	HTI	29 October 2013
Machine Vision for Mechatronic Systems	2	HTI	21 March 2013
Electronics for Non-Electronic Engineers	10	HTI	3 September 2013
Modern Optics for Optical Designers	10	HTI	13 September 2013
Tribology	4	MC	6 March 2013 (Utrecht) 4 April 2013
Introduction in Ultra High and Ultra Clean Vacuum	4	HTI	4 March 2013
Experimental Techniques in Mechatronics	3	HTI	9 April 2013
Design for Ultra High and Ultra Clean Vacuum	4	HTI	8 April 2013
Advanced Motion Control	5	HTI	7 October 2013
Cooling of Electronics Workshop	3	HTI	29 May 2013
Advanced Mechatronic System Design	6	HTI	to be planned

DSPE Certification Program

Precision engineers with a Bachelor's or Master's degree and with 2-10 years of work experience can earn certification points by following selected courses. Once participants have earned a total of 45 points (one point per course day) within a period of five years, they will be certified. The CPE certificate (Certified Precision Engineer) is an industrial standard for professional recognition and acknowledgement of precision engineering-related knowledge and skills. The certificate holder's details will be entered into the international Register of Certified Precision Engineers.

WWW.DSPEREGISTRATION.NL/LIST-OF-CERTIFIED-COURSES

Course providers

- The High Tech Institute (HTI)
WWW.HIGHTECHINSTITUTE.NL
- Mikrocentrum (MC)
WWW.MIKROCENTRUM.NL
- Dutch Society for Precision Engineering (DSPE)
WWW.DSPE.NL

UPCOMING EVENTS

26-27 February 2013, Veldhoven (NL)

RapidPro 2013

The annual event for the total additive manufacturing, rapid prototyping and rapid tooling chain.



WWW.RAPIDPRO.NL

26 February – 1 March 2013,
Ede/Veenendaal (NL)

Demoweeek 2013

Nine companies, including Heidenhain, Mitutoyo and Cellro, demonstrate their automation offerings for the metalworking industry: software, robotisation, control, measurement, 3D printing and machining.

WWW.DEMOWEEK.NL

7 March 2013, Delft (NL)

ZIE 2013

The Zuid-Holland Instrumentation Event 2013 is organised by Holland Instrumentation, a newly established network of CEOs/CTOs from high-tech companies, institutes and universities in the Dutch province of Zuid-Holland, aimed at promoting the region's instrumentation industry.



WWW.HOLLANDINSTRUMENTATION.NL

20-21 March 2013, Milton Keynes (UK)

Lamdapap 2013

Event focused on laser metrology, machine tool, CMM and robotic performance.

WWW.LAMDAPAP.COM

16 April 2013, Enschede (NL)

Industrial Laserevent 2013

Research institutes, suppliers and users exchange information on the latest developments in laser material processing.

WWW.INDUSTRIAL-LASEREVENT.NL

17-18 April 2013, 's-Hertogenbosch (NL)

Mocon 2013

Dutch trade show for motion control, drives and industrial automation. The latest innovations in design, construction, maintenance and use of components and systems will be displayed.

WWW.EASYFAIRS.COM/MOCON-NL

24-25 April 2013, Eindhoven (NL)

High-Tech Systems 2013

New event building on High Tech Mechatronica. See page 36 for a preview.

WWW.HIGHTECHSYSTEMS.NL

22-23 May 2013, Veldhoven (NL)

Vision & Robotics 2013 / RoboNED Conference 2013

The 12th edition of the Vision & Robotics trade fair and conference once again will be combined with the RoboNED conference (on Tuesday 22 May 2013). Vision & Robotics targets everyone in the Netherlands and Belgium active in the fields of vision, robotics and industrial automation. RoboNED, as one of the Dutch ICT Innovation platforms, coordinates robotics activities in the Netherlands.

WWW.VISION-ROBOTICS.NL

WWW.ROBONED.NL

27-31 May 2013, Berlin (DE)

euspenn 13th International Conference and Exhibition

Conference topics will include:

- Renewable Energy Technologies (progress enabled by precision engineering advancements)
- Nano & Micro Metrology
- Ultra Precision Machines & Control
- High Precision Mechatronics
- Ultra Precision Manufacturing & Assembly Processes
- Important/Novel Advances in Precision Engineering & Nano Technologies

WWW.BERLIN2013.EUSPEN.EU

4-5 June 2013, Veldhoven (NL)

Materials 2013, engineering & technology

New trade fair, with exhibition and lecture programme, targeted at product developers, constructors and engineers to inform them on materials innovations and applications.



WWW.MATERIALENBEURS.NL

24-28 June 2013, Eindhoven (NL)

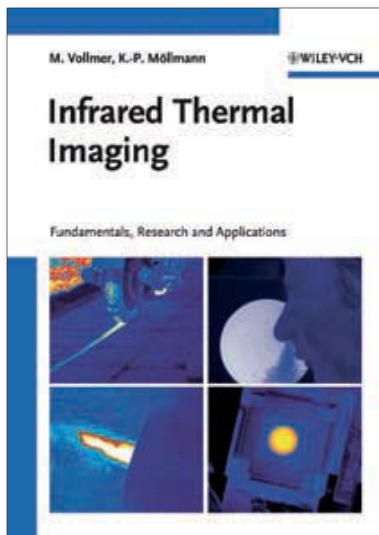
International Summer school Opto-Mechatronics 2013

Five days of intensive training, organised by DSPE and The High Tech Institute.



WWW.SUMMER-SCHOOL.NL

Book review



■ Michael Vollmer and Klaus-Peter Möllmann, "Infrared Thermal Imaging – Fundamentals, Research and Applications", Wiley-VCH, Weinheim (DE), ISBN 978-3-527-40717-0, 2011

"Infrared Thermal Imaging"

Modern industry microsystems and optics technology, as well as micro- and precision machining, are still struggling with the adverse effects of specific thermo-physical phenomena. For most technicians in these advanced fields, the adage "The numbers tell the tale" is all too familiar. Measuring technology has lately been enriched by several processes, such as computer tomography (X-raying) and, more recently, by a thermal version. However, measuring thermal conditions in this particular case is fairly difficult in practice, mainly because until recently, most of the electromagnetic effects in the infrared (IR) were invisible to the naked eye, let alone it being possible to measure them quantitatively on a reliable scale. At the start of the 21st century, dedicated R&D work resulted in a wide range of specific detector arrays, special optics, hardware and software and camera systems to upgrade the human eye.

This hardcover, richly illustrated hands-on guide is specifically written in an understandable style for practitioners in the field of IR imaging, for physics and science teachers and for researchers. The authors – both professors at the University of Applied Sciences Brandenburg (Germany) – comment: "There is today the paradox of more cameras being sold worldwide than there are technicians understanding the physics behind them, let alone being able to properly interpret the colourful images generated."

To be able to make optimum use of the book, it is absolutely essential that the authors provide deeper insights into the fundamentals of IR imaging, aside from the basic properties, the systems used, the various heat transfer concepts and advanced methodology. More than half the book covers basic applications, starting with those for direct visualisation of physics phenomena in teaching, followed by buildings and infrastructure, industrial gas detection, advanced microsystems, topics in research and industry, and finally, selected applications in other fields such as medicine, sports and art.

It is one of the first publications to include a section on microsystems. These rather delicate systems impose particular requirements on thermal imaging, such as the need for improved thermal stability, a milli-Kelvin temperature range, high-speed recording and analysis functions. This makes rapid and non-contact tracing of heat accumulation – or hot spots – possible, even in the smallest and most intricate elements. These IR measurements will give a clear indication that something is running out of control and that a breakdown is imminent. Alternatively, they could also help to discover hidden faults. These measurements thus help to optimise the lifecycle of precious machine tools, precision mechanisms and apparatus.

Kennis verbreden en verdiepen

www.cursus.paotechniek.nl

Kunststofcomposieten: Basismodule Mechanica
14 en 21 maart 2013

Mastercollegeserie: Vermogenslektronica; Advanced Topics
22 april, 6, 13, 27 mei, 3, 10, 17 en 24 juni 2013

Lijmen als verbindingstechniek
12, 13 en 14 juni 2013

Lichtgewicht Construeren voor Ontwerpers
november 2013

Postbus 5048
2600 GA Delft

Kijk voor alle cursussen op www.cursus.paotechniek.nl

015 278 83 50
info@paotechniek.nl

PAO Techniek
Opleidingen en cursussen



ESI embedded in TNO

Several everyday thermal phenomena are now within reach, encouraged by rapidly dropping prices on the market, by operator-friendly practical visualisation and general analysis tools. A broad selection of highly functional and comparatively low-priced, reliable and compact IR cameras featuring high resolution (e.g. 640 x 480 pixels up to new dimensions of 1280 x 1024) – for both thermal phase pictures (standard temperature range: –20 °C to 900 °C, up to 2,000 °C maximum) and visible video images – are available. Even picture-in-picture overlay is often a normal and most useful procedure. This makes multispectral thermography industrially and commercially more affordable – even for a high-end consumer, to detect energy losses for example – in an ever-expanding range of scientific, industrial, military, medical and commercial applications. A rather new and very interesting emerging industrial field is that of the detection of gaseous species.

Even the specialised reader finds extensive background knowledge of a great deal of aspects in a wide field of application domains. The specific contents of the cases discussed give readers, as technicians, an additional tool which they can use to select cases that suit their everyday needs.

(review by Jan Wijers, (micro) production technology freelancer, W.I.S.E. 2000 Eindhoven)

As of 1 January, the Embedded Systems Institute (ESI) has been integrated in TNO as Embedded Systems Innovation by TNO. According to a press release, the ESI expertise is a major enhancement of the TNO efforts in the field of design and engineering of software-intensive high-tech systems. The intensive cooperation with the Dutch high-tech industry, in a broad programme of research and knowledge valorisation,

and the strong anchoring of the ESI activities within the fundamental research of Dutch and foreign (technical) universities remains. TNO wants to expand in the field of system innovation in software-intensive high-tech systems. Key drivers include the “Internet of Things”, Cooperative Driving, Smart Grids and Sensor-Based Environmental Monitoring.

WWW.TNO.NL WWW.ESI.NL

TU Delft Robotics Institute launched

Last month, the TU Delft Robotics Institute was officially launched. The institute of Delft University of Technology strives to introduce novel robotics technology that will enable robots to work together with humans in human environments, contributing to all kinds of services and labour beyond “confined” industrial environments. Interdisciplinary research will address all aspects of modern robotics, drawing upon both the “hard” robot disciplines (mechatronics, embedded systems, control and Artificial Intelligence) and the “soft” robot sciences (human-machine interaction, user interaction, architecture, ethics and design). Areas of expertise are bio-inspired robot design, human-robot interaction, functional decomposition, cybernetics, spatial presence, autonomous control and machine learning.

ROBOTICS.TUDELFT.NL

Compact coordinate measuring machine

With its MICURA coordinate measuring machine, Carl Zeiss wants to meet user demands for smaller coordinate measuring machines that are as accurate as their larger relatives but offer a price advantage. This measuring machine is considerably more affordable thanks to the smaller measuring range (500 x 500 x 500 mm³). In industrial manufacturing parts, such as artificial hips, gear

wheels, optical lens elements and shafts with narrow tolerances, are becoming increasingly compact while the requirements on accuracy are rising. MICURA provides the measuring technology needed to complete these jobs, according to a press release. Measuring accuracy is below one micrometer.

WWW.ZEISS.COM



Bearing and Linear Technology



Schaeffler Nederland B.V.

Schaeffler Nederland B.V.
Gildeweg 31
3771 NB Barneveld
T +31 (0)342 - 40 30 00
F +31 (0)342 - 40 32 80
E info.nl@schaeffler.com
W www.schaeffler.nl

Schaeffler Group - LuK, INA and FAG - is a world wide leading company in developing, manufacturing and supplying of rolling bearings, linear systems, direct drives and maintenance products. Applications: automotive, industrial and aerospace.

Development



TNO
T +31 (0)88-866 50 00
W www.tno.nl

TNO is an independent innovation organisation that connects people and knowledge in order to create the innovations that sustainably boost the competitiveness of industry and wellbeing of society.

Development and Engineering



ACE ingenieurs- & adviesbureau
werktuigbouwkunde en
elektrotechniek BV
Dr. Holtropalaan 25
5652 XR Eindhoven
T +31 (0)40 - 2578300
F +31 (0)40 - 2578397
E info@ace.eu
W www.ace.eu

ACE has developed into a leading engineering and consultancy firm with a strong focus on mechanics and mechatronics. Services include conceptualization, development, engineering and prototyping.

member **DSPE**

Education



Leiden school for Instrument-makers (LiS)
Einsteinweg 61
2333 CC Leiden
The Netherlands
T +31 (0)71-5581168
F +31 (0)71-5681160
E info@lis-mbo.nl
W www.lis-mbo.nl

The LiS is founded in 1901 by the famous scientist prof. Kamerlingh Onnes. Nowadays the LiS is a modern school for vocational training on level 4 MBO-BOL. The school encourages establishing projects in close cooperation with contractors and scientific institutes, allowing for high level "real life" work.

member **DSPE**

Education



PAO Techniek
Stevinweg 1, 2628 CN Delft
Postbus 5048, 2600 GA Delft
T +31 (0)15 27 88 350
F +31 (0)15 27 84 619
E info@paotechniek.nl
W www.cursus.paotechniek.nl

Lasers and Light



Laser 2000 Benelux C.V.
Voorbancken 13a
3645 GV Vinkeveen
Postbus 20, 3645 ZJ Vinkeveen
T +31(0)297 266 191
F +31(0)297 266 134
E info@laser2000.nl
W www.laser2000.nl

Laser 2000 Benelux considers it her mission to offer customers the latest available photonics technologies.

Our areas of expertise:

- Lasers and laser systems for industry and research
- Light metrology instruments for LED and luminaire industry
- Piezo- and stepper motion products for nano- and micropositioning
- LED illumination and high speed inspection in machine vision

Laser Systems



Applied Laser Technology
De Dintel 2
5684 PS Best
T +31 (0)499 375375
F +31 (0)499 375373
E techsupport@alt.nl
W www.alt.nl

member **DSPE**



TRUMPF Nederland B.V.
Oude Boekeloseweg 31
7553 DS Hengelo
Postbus 837
7550 AV Hengelo
T +31 (0)74 2498498
F +31 (0)74 2432006
E info@nl.trumpf.com
W www.nl.trumpf.com

member **DSPE**

3D Measurement Services



Mitutoyo Nederland B.V.
Storkstraat 40
3905 KX Veenendaal
T +31 (0)318-534911
F +31 (0)318-534811
E info@mitutoyo.nl
W www.mitutoyo.nl



We make it visible.

Carl Zeiss
Industrial Metrology
Trapezium 300
3364 DL Sliedrecht
T +31 (0)184 433 551
F +31 (0)184 433 500
E m.trupia@zeiss.nl
W http://www.zeiss.nl

Carl Zeiss Industrial Metrology is the world's leader in CNC coordinate measuring machines and complete solutions for multidimensional metrology in the metrology lab and production environment. We also provide contract programming and contract measuring in our newly founded Measuring House near Eindhoven (NL).

Mechatronics Development



centre for concepts in mechatronics

CCM Centre for Concepts in Mechatronics

De Pinckart 24
5674 CC Nuenen
T +31 (0)40 2635000
F +31 (0)40 2635555
E info@ccm.nl
W www.ccm.nl

CCM translates technology into technique. Commitment, motivation, education and skills of our employees are the solid basis for our business approach.

member **DSPE**

Metal Precision Parts



Etchform BV
Arendstraat 51
1223 RE Hilversum
T +31 (0)35 685 51 94
F info@etchform.com
W www.etchform.com

Etchform is a production and service company for etched and electroformed metal precision parts.

member **DSPE**

Micro Drive Systems



Maxon Motor Benelux

The Netherlands

Head Office
maxon motor benelux bv
De Giem 22
7547 SV Enschede

South

High Tech Campus 9
5656 AE Eindhoven
T +31 (053) 486 47 77
F +31 (053) 486 47 88
E info@maxonmotor.nl
W www.maxonmotor.nl

Belgium / Luxembourg
maxon motor benelux bv
Schaliënhoedreef 20C
2800 Mechelen - Belgium
T +32 (15) 20 00 10
F +32 (15) 27 47 71
E info@maxonmotor.be
W www.maxonmotor.be

maxon motor is the worldwide leading supplier of high precision drives and systems. When it really matters! Try us.

Micro Drive Systems



Minimotor Benelux

Belgium

Dikberd 14/6c
B-2200 Herentals
T +32 (0)14-21 13 20
F +32 (0)14-21 64 95
E info@minimotor.be

The Netherlands

Postbus 49
NL-1540 Koog a/d Zaan
T +31 (0)75-614 86 35
F +31 (0)75-614 86 36
E info@minimotor.nl
W www.faulhaber.com

Faulhaber is a leading manufacturer of miniature drive systems based on ironless micromotors with the highest power-to-volume ratio.

member **DSPE**

Micromachining



Reith Laser bv
Bijsterhuizen 24-29
6604 LK Wijchen
The Netherlands
T +31 (0)24 3787564
F +31 (0)24 3787586
E info@reithlaser.nl
W www.reithlaser.nl

For more than 22 years Reith Laser bv is the leading supplier of laser-processed products in Europe. We can offer you a great diversity of lasermaterialprocessing activities:

- Laser- (micro-) cutting
- Laser drilling
- Laser welding
- Laser micromachining

Reith Laser is active in precision industry, medical industry, aerospace, semiconductor- and automotive industry.

Motion Control Systems



Aerotech LTD
Jupiter House, Calleva Park
Aldermaston
Berkshire
RG7 8NN England
T +44 (0)118 9409400
F +44 (0)118 9409401
E sales@aerotech.co.uk
W www.aerotech.co.uk



Applied Laser Technology
De Dintel 2
5684 PS Best
T +31 (0)499 375375
F +31 (0)499 375373
E techsupport@alt.nl
W www.alt.nl

member **DSPE**



IBS Precision Engineering
Esp 201
5633 AD Eindhoven
T +31 (0)40 2901270
F +31 (0)40 2901279
E info@ibspe.com
W www.ibspe.com

IBS Precision Engineering is a high-tech company in precision metrology components, systems and machines. Our solutions include special metrology machines, machine tool calibration systems, non-contact measuring systems and porous media air bearings.

member **DSPE**

Motion Control Systems



Newport Spectra-Physics B.V.
 Vechtensteinlaan 12 - 16
 3555 XS Utrecht
 T +31 (0)30 6592111
 E netherlands@newport.com
 W www.newport.com

Newport Spectra-Physics BV, a subsidiary of Newport Corp., is a worldwide leader in nano and micropositioning technologies.

member **DSPE**



Reliance Precision Mechatronics
 Florijnstraat 20
 4879 AH Etten-Leur
 The Netherlands
 T +31 (0)76 5040790
 F +31 (0)76 5040791
 E sales@rpmechatronics.co.uk
 W www.rpmechatronics.co.uk

- Positioning systems
- Drives
- Standard components
- Mechatronic assemblies

Manufacturer of among others: gears, rack, couplings and linear systems

Motion Control Systems



Rotero Holland bv
 Pompmolenlaan 21
 3447 GK Woerden
 Postbus 126
 3440 AC Woerden
 T +31 (0)348 495150
 F +31 (0)348 495171
 E info@rotero.com
 W www.rotero.com

Rotero is specialized in small electrical motors and mechanical drives. Products: AC-, DC-, stepper- and servo motors up to 1.5 kW, actuators and small leadscrews.

Optical Components



Applied Laser Technology
 De Dintel 2
 5684 PS Best
 T +31 (0)499 375375
 F +31 (0)499 375373
 E techsupport@alt.nl
 W www.alt.nl

member **DSPE**

Optical Components



Molenaar Optics
 Gerolaan 63A
 3707 SH Zeist
 Postbus 2
 3700 AA Zeist
 T +31 (0)30 6951038
 F +31 (0)30 6961348
 E info@molenaar-optics.nl
 W www.molenaar-optics.eu

member **DSPE**

Piezo Systems



Applied Laser Technology
 De Dintel 2
 5684 PS Best
 T +31 (0)499 375375
 F +31 (0)499 375373
 E techsupport@alt.nl
 W www.alt.nl

member **DSPE**

Piezo Systems



Heinmade B.V.
 High Tech Campus 9
 5656 AE Eindhoven
 T +31 (0)40 8512180
 F +31 (0)40 7440033
 E info@heinmade.com
 W www.heinmade.com

HEINMADE develops and supplies piezo system solutions for positioning and vibration damping. HEINMADE cooperates with and is distributor of Nanomotion, Noliac and Piezomechanik.

Technical Ceramics



Ceratec Technical Ceramics BV
 Poppenbouwing 35
 4191 NZ Geldermalsen
 T +31 (0)345 580101
 F +31 (0)345 577215
 E ceratec@ceratec.nl
 W www.ceratec.nl

Ceratec has specialized in industrial components constructed from technical ceramics since 1983. Ceratec's strength lies in the total formula of problem analysis, development, prototyping and production. Ceratec has modern production facilities for processing technical ceramics.

member **DSPE**

YOUR COMPANY PROFILE IN THIS GUIDE?

Please contact:

Sales & Services / Gerrit Kulsdom / +31 (0)229 211 211 / gerrit@salesandservices.nl

Dutch Society for Precision Engineering

DSPE

YOUR PRECISION PORTAL

**Your button or banner
on the website
www.DSPE.nl?**

The DSPE website is the meeting place for all who work in precision engineering.

The Dutch Society for Precision Engineering (DSPE) is a professional community for precision engineers: from scientists to craftsmen, employed from laboratories to workshops, from multinationals to small companies and universities.

If you are interested in a button or banner on the website www.dspe.nl, or in advertising in Mikroniek, please contact Gerrit Kulsdom at Sales & Services.

T: 00 31(0)229-211 211 ■ E: gerrit@salesandservices.nl

ADVERTISERS INDEX

■ Aerotech Ltd	37
www.aerotech.com	
■ Ceratec	42
www.ceratec.nl	
■ Heidenhain Nederland BV	56
www.heidenhain.nl	
■ High-Tech Systems 2013	Leaflet, 2
www.hightechsystems.eu	
■ Mikroniek Guide	52-54
■ Minimotor Benelux	20, 29
www.faulhaber.com	
■ PAO Techniek	50
www.cursus.paotechniek.nl	

DSPE

YOUR PRECISION PORTAL



MIKRONIEK

Mikroniek is the professional journal on precision engineering and the official organ of the DSPE, The Dutch Society for Precision Engineering.

Mikroniek provides current information about technical developments in the fields of mechanics, optics and electronics and appears six times a year.

Subscribers are designers, engineers, scientists, researchers, entrepreneurs and managers in the area of precision engineering, precision mechanics, mechatronics and high tech industry. Mikroniek is the only professional journal in Europe that specifically focuses on technicians of all levels who are working in the field of precision technology.

Publication dates 2013:

nr.:	deadline reservation	publication date:
2	15-03-2013	19-04-2013 - High Tech Systems
3	17-05-2013	21-06-2013 - Thermo-Mechanics
4	26-07-2013	30-08-2013
5	06-09-2013	11-10-2013 - Robotics
6	11-10-2013	22-11-2013 - (Preceding the Precision Fair)

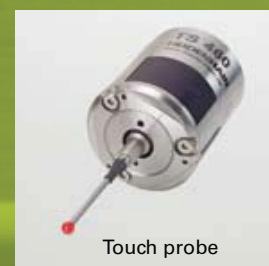
**For questions about advertising
please contact Gerrit Kulsdom**

Dial: 00 31(0)229-211 211 ■ E-mail: gerrit@salesandservices.nl



How fast is the payoff from our touch probe?

When you let a TS touch probe cross the start line, your machines quickly win productive time. It not only lets you set up your work-pieces quickly and precisely, it even inspects them between machining steps. Its optical switch, which operates without contact and therefore without wear, guarantees a consistently high probe repeatability of $\pm 1 \mu\text{m}$. So with the TS touch probes from HEIDENHAIN, your machines will work more quickly. And your race will always be a sure thing. HEIDENHAIN NEDERLAND B.V., Postbus 92, 6710 BB Ede, Telefoon: (03 18) 58 18 00, Telefax: (03 18) 58 18 70, www.heidenhain.nl, E-Mail: verkoop@heidenhain.nl



Touch probe